TDP-43 promotes tau accumulation and selective neurotoxicity in bigenic *C. elegans*

Caitlin S. Latimer[1], Jade G. Stair[2], Joshua C. Hincks[2], Heather N. Currey[2], Thomas D. Bird[2,3,4], C. Dirk Keene[1], Brian C. Kraemer[1,2,5,6], Nicole F. Liachko[2,6*]

Author emails: caitlinl@uw.edu (CSL), jadegaohao@gmail.com (JGS), joshua.c.hincks@gmail.com (JCH), hncurrey@alaska.edu (HNC), tomnroz@uw.edu (TDB), cdkeene@uw.edu (CDK), kraemerb@uw.edu (BCK), nliachko@uw.edu (NFL)

[1] Department of Laboratory Medicine and Pathology, University of Washington, Seattle, Washington 98195, USA.

[2] Geriatrics Research Education and Clinical Center, Veterans Affairs Puget Sound Health Care System, Seattle, WA 98108, USA.

[3] Department of Neurology, University of Washington, Seattle, WA 98104, USA.

[4] Division of Medical Genetics, Department of Medicine, University of Washington, Seattle, WA 98104, USA.

[5] Department of Psychiatry and Behavioral Sciences, University of Washington, Seattle, Washington 98195

[6] Division of Gerontology and Geriatric Medicine, Department of Medicine, University of Washington, Seattle, WA 98104, USA.

[*]To whom correspondence should be addressed at:
Seattle Veterans Affairs Puget Sound Health Care System
GRECC, S182, 1660 South Columbian Way, Seattle, WA 98108
Phone (206) 277-1587 Fax (206) 764-2569
Email: nliachko@uw.edu

Disease Models & Mechanisms • DMM • Accepted manuscript

Summary Statement

TDP-43 co-pathology is a frequent feature of Alzheimer's disease. We demonstrate that TDP-43 specifically enhances tau neurotoxicity but not Aβ to promote pathological protein accumulation, behavioral impairment, and selective neurodegeneration.

Abstract

While amyloid (A) β and tau aggregates define the neuropathology of Alzheimer's disease (AD), TDP-43 has recently emerged as a co-morbid pathology in over half of patients with AD. Individuals with concomitant Aβ, tau, and TDP-43 pathology experience accelerated cognitive decline and worsened brain atrophy, but the molecular mechanisms of TDP-43 neurotoxicity in AD are unknown. Synergistic interactions among Aβ, tau, and TDP-43 may be responsible for worsened disease outcomes. To study the biology underlying this process, we have developed new models of protein co-morbidity using the simple animal *C. elegans.* We demonstrate that TDP-43 specifically enhances tau but not Aβ neurotoxicity, resulting in neuronal dysfunction, pathological tau accumulation, and selective neurodegeneration. Furthermore, we find that synergism between tau and TDP-43 is rescued by loss-of-function of the robust tau modifier *sut-2*. Our results implicate enhanced tau neurotoxicity as the primary driver underlying worsened clinical and neuropathological phenotypes in AD with TDP-43 pathology, and identify cell-type specific sensitivities to co-morbid tau and TDP-43. Determining the relationship between co-morbid TDP-43 and tau is critical to understand and ultimately treat mixed pathology AD.

Keywords: TDP-43, tau, amyloid β (Aβ), *C. elegans*, Alzheimer's disease, proteotoxicity

Introduction

Alzheimer's disease (AD) is pathologically defined by the presence of extracellular amyloid (A) β plaques and intracellular tangles of hyperphosphorylated tau (ptau) [1–5]. Both Aβ and tau are implicated in AD neurodegeneration. Mutations in genes involved in the processing of amyloid precursor protein (APP) cause some cases of inherited familial AD, supporting a

mechanistic role for Aβ pathology in the disease [6]. However, tau pathology correlates best with clinical disease progression and severity [7,8]. Although mutations in the gene encoding tau have not been shown to directly cause AD, they are causal for another neurodegenerative tauopathy, frontotemporal lobar degeneration (FTLD)-tau, indicating dysfunction of tau also plays a mechanistic role in disease [9]. Numerous models of Aβ and tau proteotoxicity have been developed to study their neurotoxic effects *in vitro* and *in vivo*, and have demonstrated that Aβ and tau together have worse cognitive and neurodegenerative consequences than either pathology on its own [10]. Recent work characterizing additional co-pathologies in AD have identified a third protein, TDP-43, as a likely relevant contributor to AD pathophysiology [11–14].

TDP-43 was first identified in 2006 as the major component of pathologic inclusions in amyotrophic lateral sclerosis (ALS) and approximately 50% of cases of frontotemporal lobar dementia (FTLD-TDP) [15,16]. TDP-43 is an essential protein involved in multiple cellular processes, including alternative splicing of the majority of mRNA gene products, stabilization and transport of RNA transcripts, and the formation and stabilization of stress granules [17,18]. Like tau, TDP-43 is subjected to post-translational modifications, including phosphorylation and acetylation, that promote aggregation [19]. Although the exact mechanisms continue to be studied, cytoplasmic mis-localization, phosphorylation, and aggregation of TDP-43 contribute to neuronal dysfunction and neurodegeneration likely through both loss and gain of TDP-43 functions [20,21]. Most cases of ALS and FTLD-TDP are sporadic, without a known genetic cause. However, rare mutations in the gene encoding TDP-43, *TARDBP*, are causative for ALS, demonstrating that dysfunctional TDP-43 actively contributes to neurodegenerative pathways [22,23].

Following its identification as a key pathologic protein in ALS and FTLD-TDP, TDP-43 pathology was also found to occur as a secondary pathology in other neurodegenerative diseases [24–26]. In particular, TDP-43 co-pathology has been recognized in more than half of neuropathologically-confirmed cases of AD [12,27–34] and several large cohort studies have found that TDP-43 co-pathology is associated with significantly accelerated clinical progression in AD patients [12,35,36], including more rapid rates of cognitive decline and increased mesial temporal atrophy [37–39]. Notably, concomitant TDP-43 pathology in AD occurs more frequently as tau pathology progresses into additional brain regions, denoted by higher Braak stage. The

reported association between phosphorylated TDP-43 (pTDP-43) in hippocampus and faster hippocampal atrophy on MRI was limited to cases with higher Braak stages (III-VI) [40] suggesting tau and TDP-43 may influence each other to promote neuronal dysfunction and neurodegeneration [14,33]. In AD, neurofibrillary tangles and TDP-43 positive inclusions can co-exist or co-localize within a subset of neurons [31,41,42], with about 25% of phosphorylated TDP-43 immunopositive neurons also exhibiting pathological tau (PHF-1) immunoreactivity [42].

To date, there are limited studies exploring the relationship between tau and TDP-43 *in vitro* or *in vivo*. In cell and mouse models, TDP-43 regulates mRNA splicing of tau exon 10, shifting the ratio of tau microtubule binding repeats from the normal balanced ratio of 3R/4R-tau to a higher proportion of 4R-tau [43]. Recent work demonstrated that tau oligomers promote accumulation of cytoplasmic TDP-43 in HEK293 cells, and brain-derived TDP-43 oligomers can cross-seed tau aggregates *in vitro* [44]. In *Caenorhabditis elegans*, we have shown pan-neuronal co-expression of human tau and TDP-43 causes significant lethality, dramatically enhanced uncoordination, and an increase in accumulation of both total and phosphorylated tau and TDP-43 compared to controls expressing tau or TDP-43 alone [35]. However, the strong synthetic lethal phenotypes in this overexpression model preclude its use studying underlying causative relationships.

In order to dissect TDP-43 synergism with other pathological proteins, we have developed new refined models of comorbid TDP-43 with the AD proteins tau and Aβ in *C. elegans*. Using these models, we show that very low levels of TDP-43 promote tau neurotoxicity, leading to significant sensory and behavioral impairments, accumulation of pathological phosphorylated tau, and selective neurodegeneration of neurons expressing specific neurotransmitter types. We further show that synergism between tau and TDP-43 is specific and does not extend to Aβ or poly-glutamine combined with TDP-43. Finally, we demonstrate that genetic loss-of-function of the tau modifier, *sut-2*, can robustly prevent the enhanced neurotoxicity and neurodegeneration observed in this model.

Results

To dissect the contribution of TDP-43 to exacerbated AD pathology-related neurotoxicity and neurodegeneration, we generated a new *C. elegans* strain with modest pan-neuronal expression of human TDP-43 (TDP Tg-low). Expression of TDP-43 in this strain is maintained at very low levels by the insertion of a self-cleaving ribozyme between the TDP-43 coding sequence and the 3'UTR of the transgene, which results in the inactivation of most, but not all transgene derived transcripts (Fig. S1)[45]. In order to test whether TDP-43 potentiates neurotoxicity of the AD proteins tau or Aβ, TDP Tg-low animals were crossed with strains expressing wild-type human tau or Aβ1-42 pan-neuronally (tau Tg or Aβ Tg, respectively) to generate the co-expression strains tau+TDP Tg-low and Aβ+TDP Tg-low.

TDP-43 synergizes with tau but not Aβ to worsen motility deficits

Visually, the tau+TDP Tg-low animals exhibit dramatically worse motility than either tau Tg or TDP Tg-low strains, manifested by increased uncoordination in their movement. In fact, impaired motility has been used successfully as a readout for neuronal dysfunction or neurodegeneration in other *C. elegans* models of neurodegenerative disease [46,47] and represents the reciprocal functionality of both GABA-ergic and cholinergic neurons in motor circuits. To measure the severity of tau+TDP Tg-low uncoordination, we utilized automated video tracking to assay two different movement paradigms: unstimulated activity on a solid surface and thrashing in liquid. We found that these animals exhibited significantly decreased activity and worsened thrashing motility (Fig. 1a-b and Videos S1-8). In contrast, Aβ+TDP Tg-low animals exhibited no change in motility from control strains (Fig. 1c-d). To confirm these results, we generated an additional strain co-expressing a different Aβ transgene with TDP Tg-low (Aβ2+TDP Tg-low [48]). Similarly, these animals exhibited no change in motility (Fig. S2).

As controls, we examined whether tau Tg or TDP Tg-low would synergize with a non-AD related neurodegenerative disease model expressing 86 repeats of polyglutamine pan-neuronally (polyQ Tg) [49,50]. PolyQ Tg animals accumulate insoluble inclusions of polyglutamine and have significant motility dysfunction on their own (Fig. 2). We have previously been able to distinguish enhancement of motility dysfunction from already impaired strains using assays

detecting activity on a solid surface or thrashing in liquid [51,52]. In this case, we found no alteration in motility in either polyQ+tau Tg or polyQ+TDP Tg-low strains compared to controls (Fig. 2). Taken together, these experiments suggest that the neurotoxic synergy observed between tau and TDP-43 is specific rather than a non-specific enhancement of toxicity due to an increase in neuronal protein load, protein aggregation, or merely additive toxicity through two independent pathological mechanisms.

tau+TDP Tg-low animals exhibit impaired mechanosensation

We next examined several well-characterized behavioral outputs in the tau+TDP Tg-low model. Mechanosensation integrates signaling from dopaminergic, glutamatergic, and serotonergic neurotransmitter classes of neurons to generate a stereotypical response to light touch. To evaluate this, we employed an assay evaluating responses to gentle touch with an eyelash hair 10 times, alternating head and tail touches. Consistent with prior reports [53–55], tau Tg animals had a moderate defect in mechanosensation (Fig. 3a). Interestingly, we found that tau+TDP Tg-low animals had significantly worsened defects in mechanosensation. We also tested whether tau+TDP Tg-low animals had altered pharyngeal pumping (feeding behavior), an activity that integrates signaling from serotonergic, octopaminergic, and cholinergic neurotransmitter classes of neurons. To assay this, we employed microfluidic electropharyngeogram (EPG) recording to measure electrical currents emitted by pharyngeal muscles and neurons [56,57]. However, we did not observe any significant effects on the frequency or duration of pharyngeal pumping in tau+TDP Tg-low (Fig. 3b-d), indicating the circuits controlling this behavior remain intact.

TDP-43 promotes increased accumulation of total and phosphorylated tau

It is possible that the motility and sensory impairments observed in tau+TDP Tg-low are due to accumulation of neurotoxic pathological tau or TDP-43. To determine whether the co-expression of tau and very low levels of TDP-43 influenced their protein accumulation, we measured protein levels in tau+TDP Tg-low by immunoblot. We found that both total and phosphorylated tau increased in tau+TDP Tg-low (Fig. 4a-c), but surprisingly, protein

accumulation of TDP-43 was unchanged from TDP-43 Tg-low alone and there was no apparent accumulation of phosphorylated TDP-43 (Fig. 4a,d-e). We tested whether differences in tau protein levels in tau+TDP Tg-low animals were due to increased mRNA expression, but we did not see any significant differences from tau Tg alone (Fig. S3). Therefore, TDP-43 potentiates pathological tau protein changes, which may be the primary driver of neurotoxicity in co-expression models of tau and TDP-43.

tau+TDP Tg-low animals exhibit selective neuronal vulnerability through aging

To determine whether the motor and sensory defects of tau+TDP Tg-low are the result of neurodegeneration, we assayed for neuronal integrity in these animals using GFP reporters specific for distinct neurotransmitter classes of neurons (dopaminergic, glutamatergic, serotonergic, cholinergic, or GABA-ergic). We also evaluated whether aging differentially affected these various neurotransmitter classes of neurons by assessing neurodegeneration over time at day 1 and day 4 of adulthood. This survey revealed distinct differences in neuron vulnerabilities by neurotransmitter class to co-morbid tau and TDP-43, and to aging. We found no significant difference in dopaminergic neurons at either day 1 or day 4 of adulthood between all strains (Fig. S4). Conversely, all transgenic strains surveyed had a significant decrease in glutamatergic neurons compared to non-Tg animals at day 1 of adulthood; however, by day 4 of adulthood, both tau Tg and tau+TDP Tg-low animals had lost significantly more neurons than non-Tg or TDP Tg-low animals alone (Fig. 5a-c). Interestingly, we saw a different pattern of loss in serotonergic neurons, where at day 1 of adulthood only tau+TDP Tg-low animals lost significantly more neurons than controls (Fig. 5d-e). By day 4 of adulthood, tau Tg animals exhibited significant neurodegeneration; however, at this age, neuron loss in tau+TDP Tg-low animals did not progress further and was not significantly different from tau Tg animals (Fig. 5f). In cholinergic and GABA-ergic type neurons still another pattern of neurodegeneration was noted. Although both tau Tg and tau+TDP Tg-low Tg animals exhibited significant cholinergic and GABA-ergic neuronal loss compared to controls at day 1 and day 4 of adulthood, the neuron loss was most severe in tau+TDP Tg-low animals at both timepoints (Fig. 6).

Loss of sut-2 prevents protein accumulation and motility deficits in tau+TDP Tg-low animals

To test whether suppression of tau toxicity can protect against the phenotypes of co-expressed tau and TDP-43, we used a CRISPR-Cas9 generated whole-gene deletion mutation in a known, well-characterized suppressor of tau, *sut-2/MSUT2* [50,58,59]. We found *sut-2* null mutations (*sut-2 (-)*) robustly protected against tau+TDP Tg-low uncoordinated motility (Fig. 7a) and GABA-ergic neurodegeneration (Fig. 7b-c). We then examined whether *sut-2(-)* could reduce the accumulation of tau or TDP-43 protein. We found that *sut-2(-)* reduced both total tau protein and pathological phosphorylated tau in tau+TDP Tg-low animals (Fig. 8a-c). However, *sut-2(-)* did not significantly reduce levels of total or phosphorylated TDP-43 in tau+TDP Tg-low (Fig. 8a,d-e). Taken together, these data suggest that enhanced tau neurotoxicity underlies the synergism observed between tau and TDP-43.

Discussion

Through a series of functional experiments in a *C. elegans* model of combined tau and TDP-43 proteotoxicity, we demonstrate that the presence of TDP-43 promotes the accumulation and hyperphosphorylation of tau, while tau does not have the same effect on TDP-43 protein. We also show that the combination of tau and TDP-43 differentially affects neurons of different neurotransmitter classes, indicating some degree of selective cell-type vulnerability. Further, we show that suppression of tau neurotoxicity using the genetic modifier *sut-2* protects against effects of tau and TDP-43 synergism.

TDP-43 promotes tau-driven neurotoxicity and neurodegeneration

The attenuated model of co-expressed tau and TDP-43 described here utilizes a TDP-43 transgene with very low pan-neuronal expression of human TDP-43, and accumulates minimal measurable phosphorylated TDP-43. Neither total nor phosphorylated TDP-43 protein levels significantly change in the combined tau+TDP-43-low Tg animals, although there may be biologically relevant differences that did not reach statistical significance in these experiments. This suggests that tau does not promote pathological TDP-43 protein changes as robustly as

TDP-43 enhances tau pathology and therefore, the worsened behavioral phenotypes and neurodegeneration are less dependent on increased total or phosphorylated TDP-43. Conversely, the observed significant increase in both total and phosphorylated tau in the tau+TDP-43-low Tg animals indicates that low levels of non-phosphorylated wild-type TDP-43 can drive increased tau pathology with concomitant worsened neuronal function and neurodegeneration. We tested whether loss of the endogenous *C. elegans* TDP-43 homolog, *tdp-1*, impacted neurotoxicity of tau Tg animals, but did not see any difference in tau-mediated motility dysfunction (Fig. S5). The *C. elegans tdp-1* gene lacks the C-terminal G-rich domain present in human TDP-43, which is the site of pathological phosphorylation, the location of most ALS-causing mutations in the *TARDBP* gene, and comprises the fibrillar core of aggregates in FTLD-TDP.[60,61] It is possible that this C-terminal domain is a critical region involved in synergy with tau. The relationship between tau and TDP-43 is likely complex, and while these results do not exclude a reciprocal effect of tau on TDP-43, they do support TDP-43 promoting tau-driven neurotoxicity and neurodegeneration as a major component of the underlying mechanism.

Previous studies evaluating a potential relationship between tau and TDP-43 have suggested that tau initiates TDP-43 pathology [62]. While this relationship is not observed in tau+TDP Tg-low animals, our previous, more severe model employing higher co-expression of tau and TDP-43 did show a strong increase in both total and phosphorylated tau and TDP-43 protein. These differences may be due to a threshold effect, below which tau does not impact TDP-43, and above which it reciprocally enhances TDP-43 pathology. Additional work is necessary to further tease apart these complex pathological protein interactions.

Neurotransmitter classes of neurons are selectively vulnerable to comorbid tau and TDP-43

We find that different neurotransmitter classes of neurons are selectively vulnerable to co-expression of tau and TDP-43. Dopaminergic neurons were resistant to tau and TDP-43, while glutamatergic, serotonergic, cholinergic, and GABA-ergic neurons all exhibited worsened neuronal loss. Interestingly, these neuron classes also exhibited differences through aging and among neurotransmitter class. In glutamatergic neurons, tau Tg and tau+TDP Tg-low animals had similar degrees of neurodegeneration over time, indicating TDP-43 does not worsen tau-

driven neuronal loss in these cells. In serotonergic neurons, TDP-43 appears to accelerate early tau-driven neurodegeneration, but not worsen the total neurodegeneration accumulating over time. Finally, co-expression of tau and TDP-43 in cholinergic and GABA-ergic neurons led to significantly increased neuronal loss at each time point surveyed. Although it is possible that differences in *snb-1* or *aex-3* expression among these neurotransmitter classes may underlie the observed vulnerabilities, we do not believe this is the case, as both *snb-1* and *aex-3* are robustly expressed across neurons, including dopaminergic neurons which were resistant to combined tau+TDP.[63] There have been considerable efforts made to understand the selective vulnerability of neurons to different pathologic processes in neurodegenerative diseases including AD[64]. In terms of the various neurotransmitter classes, evidence suggests that all are to some degree affected in AD, but the underlying mechanisms driving their vulnerabilities, and the temporal patterns of their involvement, are poorly understood.

Dysfunction of both glutamatergic and cholinergic neurons in AD is well described[65,66]. Glutamate, the primary excitatory neurotransmitter in the human brain, has been shown to decrease both with age and AD pathology[67,68]. Similarly, cholinergic synapses have long been implicated in the pathophysiology of AD given their prominence throughout the limbic system and neocortex, regions that coincide with both progressive tau and TDP-43 pathology[69,70]. In our model, the cholinergic neurons of animals with both tau and TDP-43 were more significantly affected than those with either tau or TDP-43 alone at both ages.

Although less well studied, GABA-ergic neurons have more recently been shown to play a role in AD. GABA-ergic neurons are involved in cortical microcircuits that are affected in AD, and increasing evidence supports AD deficits linked to GABA-ergic inhibitory neuron dysfunction [71–73]. The serotonergic system is also implicated in AD[74,75] and some studies suggest that loss of serotonergic input is associated with early behavioral changes in AD, including increased agitation and loss of emotional regulation, clinical features that manifest before the later onset of memory loss and may also correlate with concomitant TDP-43 pathology[76–78]. Although cell type vulnerability observed in our model is intriguing, further characterization of tau and TDP-43 pathology in these neuronal subtypes in human brain tissue

will be necessary to better understand both the relevance of the model and the pathophysiology of the human disease.

The synergistic relationship between tau and TDP-43 is specific

To determine the specificity of the neurotoxic synergy observed between tau and TDP-43, we tested whether TDP-43 could synergize with Aβ, another pathological AD protein. However, the Aβ+TDP Tg animals showed no enhancement of movement impairment compared to the lowest motility single transgenic strain (either TDP-43 or Aβ Tg animals). Notably, it has been previously shown that tau synergizes with Aβ in *C. elegans* using the same transgenes used here (tau Tg and Aβ Tg) [79]. We also tested whether a neurotoxic non-AD neurodegenerative disease-associated protein, 86 repeats of poly-glutamine, could synergize with tau or TDP-43. However, we did not observe any enhancement of movement impairment in polyQ+tau Tg or polyQ+TDP Tg-low compared with polyQ Tg alone. Taken together, these data support the idea that tau and TDP-43 have a biologically relevant interaction, and therefore, the phenotypes observed in tau+TDP Tg animals are not simply due to neuronal protein load or non-specific additive toxicities of two distinct pathologic proteins.

Interestingly, in our models of co-expressed Aβ and TDP-43, we see no evidence of synergism between them. There is limited data on potential relationships between TDP-43 and Aβ reported in the literature, which includes some human autopsy studies. In a predictive model of neuropathological pathways, neuritic amyloid plaques had a significant effect on TDP-43 pathology [80]. However neuritic plaques represent a combined lesion that includes both pathologic tau and Aβ, as well as more advanced disease. Data associating TDP-43 with diffuse Aβ pathology irrespective of tau is not reported and indeed, a study examining TDP-43 pathological correlates with antemortem Aβ found no association with global amyloid PET signal [81]. In experimental systems, *in vitro* TDP-43 does not modulate the expression of APP, nor does APP affect TDP-43 expression [82], but TDP-43 can accelerate Aβ aggregation in an *in vitro* seeding assay [83]. In a separate study, injection of TDP-43 into brains of a transgenic mouse model of AD β-amyloidosis altered β-amyloid assembly and increased accumulation of toxic β-

amyloid oligomers [84]. Thus, the relationship between TDP-43 and Aβ necessitates further investigation.

Loss of the potent tau modifier sut-2/MSUT2 prevents tau and TDP-43 synergistic neurotoxicity

In studies evaluating the role of *sut-2/MSUT2* in cell culture, *C. elegans,* and mouse models of tau neurotoxicity, genetic loss of *sut-2* protects against accumulation of insoluble tau, and prevents tau-mediated behavioral and cognitive decline and neurodegeneration [50,59,85]. Here, we find loss of *sut-2* also suppresses the neurotoxicity of co-expressed tau and TDP-43. *sut-2(-)* only modestly decreases TDP-43 protein accumulation and does not protect against TDP Tg motility impairment. The near complete amelioration of motility defects and neurodegeneration in the combined tau+TDP-low Tg model in the presence of the tau suppressor *sut-2(-)* supports the concept that enhanced tau neurotoxicity drives the exacerbated phenotypes. However, the mechanism of this protection remains unknown. SUT-2/MSUT2 is nuclear localized, binds mRNA, and regulates poly-A tail length[50,86–88]. Loss of *sut-2* may drive increased amounts of mRNA into the cytoplasm, which can serve as a polyanion seed for tau aggregation. Loss of *sut-2* may decrease export of mRNA into the cytoplasm, reducing RNA-mediated tau aggregation and neurotoxicity[89,90].

The underlying mechanisms by which TDP-43 promotes tau pathology are not understood.

Human neuropathology data demonstrate that both tau and TDP-43 pathology occur in the same brain regions and can co-exist within the same neurons [25,26,91]. Furthermore, phosphorylated tau and TDP-43 derived from AD brain can co-immunoprecipitate, indicating a physical interaction[92]. Normal TDP-43 is predominantly localized to the nucleus and tau to the cytoplasm, making a direct interaction unlikely under homeostatic cellular conditions. However, TDP-43 can shuttle to the cytoplasm to carry out some of its physiologic functions, and redistribution of TDP-43 to the cytoplasm is believed to be an important part of the pathologic process. Classical pathological TDP-43 aggregates are found within the cytoplasm as perinuclear inclusions or other structures, in addition to intranuclear pathology. Further, although tau is

best studied for its roles in microtubule assembly and stability, it can also be found in the nucleus where it is capable of binding DNA and may stabilize heterochromatin [93]. Therefore, a direct interaction cannot be completely excluded; indeed, recent work provides compelling evidence for a direct interaction between pathological TDP-43 and pathological tau [92] and prior ultrastructural studies have shown TDP-43 within tau structures in neurons, both in animal models and human tissues [62,94]. Determining whether individual domains of TDP-43 contribute to this synergy will be important future work.

Aside from a direct interaction, TDP-43 has multiple roles that could ultimately impact tau and tau pathology more indirectly, such as regulation of RNA splicing[95]. TDP-43 directly binds to and regulates the splicing of most cellular pre-mRNAs, including tau mRNA, which has been shown to alter the ratio of tau isoforms implicated in neurodegenerative disease and may represent one mechanism of tau pathology exacerbation [96]. More extensive work in this model system and others are needed to further investigate the mechanism of TDP-43 enhancement of tau pathology.

TDP-43 may act through additional pathways unrelated to tau pathology

In addition to enhancing tau pathology, TDP-43 can promote neurodegeneration through separate, tau-independent pathways. In human diseases, there are primary TDP-43 proteinopathies, such as ALS and FTLD-TDP, which are characterized by TDP-43 pathology in the absence of tau pathology. Mutations in the gene coding for TDP-43 cause some cases of ALS [97] and numerous animal models have shown aberrant TDP-43 promotes neurodegeneration [98]. Our model of combined tau and TDP-43 illustrates that while TDP-43 is capable of causing neurodegenerative changes on its own, when tau is present, it can additionally act to exacerbate tau pathology and set into motion a neurodegeneration cascade more severe than if either protein were present alone.

Tau and TDP-43 synergy represents a novel therapeutic target for treating AD

There is a great clinical need for effective AD therapeutics, as currently there are no treatments that arrest disease progression in AD. Co-morbid TDP-43 occurs in over half of patients with AD, and correlates with more severe disease course and greater neurodegeneration. We have shown that TDP-43 selectively enhances tau neurotoxicity, providing a possible mechanism for the clinical impact of TDP-43 in AD. Because the underlying mechanisms may be distinct, it is possible that the treatment for patients with both AD and TDP-43 pathology will need to be different from those for patients that lack this comorbidity. Modulation of the tau suppressor *MSUT2* may be another viable target to intervene in AD with co-morbid TDP-43. A therapy that reduced or prevented TDP-43 and tau synergy could represent a novel and effective strategy to treat AD. To achieve this, continued development and testing of experimental models that incorporate multiple pathological proteins, and in particular TDP-43, is essential. These models will allow a deeper understanding of underlying mechanisms, as well as a system to test AD-targeting interventions.

Conclusions

The role of pathological TDP-43 in AD is only just now becoming widely appreciated despite published neuropathologic descriptions dating back to 2006, and there are few published models of this combined pathology. Here we demonstrate that modeling co-morbid tau and TDP-43 is relevant and necessary for advancing our understanding of the proteotoxic pathways underlying AD. We show that TDP-43 can exacerbate tau pathology, setting into motion a neurodegeneration cascade more severe than if either protein were present alone, and dependent on the neuron subtype. The robust amelioration of the combined phenotype by the loss of function of a known potent tau modifier, *sut-2/MSUT2*, further supports the notion that the enhanced phenotype is largely due to a TDP-43-driven exacerbation of tau pathology. Our extensive characterization of this *C. elegans* model of tau and TDP-43 co-expression provides a baseline upon which to build and improve our understanding of how these proteins interact to exacerbate neurodegenerative pathways. Synergy between tau and TDP-43

represents a novel therapeutic target for AD with TDP-43 pathology. Continued work using simple and translational models will be crucial for further probing those mechanisms and identifying treatment strategies.

Materials and Methods

C. elegans strains and transgenics

Wild-type *C. elegans* (Bristol strain N2) was maintained as previously described [99]. Previously generated transgenic strains used were CK1441 *bkIs1441[Paex-3::Tau WT(4R1N)+Pmyo-2::dsRED]* [79], GRU102 *gnaIs2[Pmyo-2::YFP+Punc-119::Abeta1-42]* [48], CL2355 *dvIs50[pCL45(snb-1::Abeta1-42::3'UTR(long) + mlt-2::GFP]* [100], CK241 *bkIs241[pF25B5.3::Q86-YFP]* [50], and EG1285 *oxIs12*[P*unc-47*::GFP *+ lin-15(+)*] [101]. CK1943 *bkIs1943[Psnb-1::hTDP-43 WT::K4aptazyme::unc-54 3'UTR+Pmyo-3::mCherry]* was generated using a transgene with the K4 aptazyme sequence (a fusion RNA of a type III hammerhead ribozyme with a tetracycline binding RNA aptamer[45,102]) between the wild-type human TDP-43 cDNA and 3'UTR. Multicopy integrated transgenes were produced using germline microinjection, integration, and outcrossing as previously described in [45,102]. NLS19 *bkIs1441[Paex-3::Tau WT(4R1N)+Pmyo-2::dsRED]; bkIs1943[Psnb-1::hTDP-43 WT::K4aptazyme::unc-54 3'UTR+Pmyo-3::mCherry]* was generated by crossing CK1441 and CK1943. The CRISPR generated whole gene deletion CK3011 *sut-2(bk3011)* was generated as described in [86]. Strain NLS19 was crossed with CK3011 *sut-2(bk3011)* to generate NLS23 *sut-2(bk3011); bkIs1441[Paex-3::Tau WT(4R1N)+Pmyo-2::dsRED]; bkIs1943[Psnb-1::hTDP-43 WT::K4aptazyme::unc-54 3'UTR+Pmyo-3::mCherry]*, NLS24 *sut-2(bk3011); bkIs1943[Psnb-1::hTDP-43 WT::K4aptazyme::unc-54 3'UTR+Pmyo-3::mCherry]*, and NLS25 *sut-2(bk3011); bkIs1441[Paex-3::Tau WT(4R1N)+Pmyo-2::dsRED]*. Strains with GFP marked serotonergic neurons were generated by crossing the reporter strain JPS617 [P*tph-1*::GFP] with CK1441, CK1943, and NLS19. Strains with GFP marked dopaminergic neurons were generated by crossing the reporter strain WG1 [P*dat-1*::GFP] with CK1441, CK1943, and NLS19. Strains with GFP marked glutamatergic neurons were generated by crossing the reporter strain OH10972 [P*eat-4*::GFP] with CK1441, CK1943, and NLS19. Strains with GFP marked cholinergic

neurons were generated by crossing the reporter strain LX929 [P*unc-17*::GFP] with CK1441, CK1943, and NLS19. Strains with GFP marked gamma-aminobutyric acid (GABA)-ergic motor neurons were generated by crossing *sut-2(bk3011)* with CK1441, CK1943, NLS19, and the reporter strain EG1285 [P*unc-47*::GFP].

Motility assays

Unstimulated activity and thrashing behaviors were assessed using the WormLab system (MBF Bioscience). For unstimulated activity assays, stage matched day 1 adult *C. elegans* were transferred to 35mm NGM assay plates seeded with 20µL OP-50 bacteria. Animals were allowed to acclimate to conditions on assay plates at room temperature for at least 30 minutes before recording movements for 1 minute at 7.5 frames per second. For thrashing assays, staged matched day 1 adult *C. elegans* were given 30 minutes to acclimate to the assay room conditions. Approximately 50 animals were then transferred to a 35mm assay plate by way of washing in 1mL M9 buffer, given 1 minute to standardize swimming behavior, followed by a 1 minute recording time at 14 frames per second. Tracks were verified and repaired as needed. Figures show results from at least 3 independent replicates.

Mechanosensation assay

Mechanosensation assays were adapted from Miyasaka, T. *et al.*[53]. In brief, an eyelash was gently touched across the anterior and posterior of each day 1 adult worm successively five times each, for a total of ten touches per trial. Touch responses were summarized on a 0-2 scale (2: normal response, 1: abnormal response, and 0: no response). Fifteen worms of each strain were scored per independent replicate for a total of forty-five worms per genotype. Scoring was conducted blinded to genotype. Figures show results from 3 independent replicates.

EPG assay

Electropharyngeogram (EPG) comparisons were performed using the NemaMetrix ScreenChip System and associated software packages NemAquire and NemAnalysis, and Microsoft Excel. Stage-matched day 1 adult animals were washed in M9 and then incubated at

room temperature in 10mM Serotonin in M9 buffer for 20 minutes to induce pharyngeal pumping. Animals were loaded into a ScreenChip20 cartridge under vacuum. The electrical signal (which is driven primarily by pharyngeal pumping) was recorded individually for 2 minutes. Average pump frequency and duration readouts from NemAnalysis were averaged over 3 independent replicates per strain.

Neurodegeneration assays

Animals were grown to day 1 or day 4 adult. Living animals were immobilized on a 2% agarose pad with 0.01% sodium azide, and intact neurons were scored under fluorescence microscopy on a DeltaVision Elite (GE, Issaquah, WA) imaging system using an Olympus 60x oil objective. Scoring was conducted blinded to genotype. Figures show results from at least 3 independent replicates.

Immunoblotting and quantitation

Approximately 10,000 stage-matched day 1 adult *C. elegans* were harvested and snap frozen per sample. Protein was extracted by resuspending pellets in 1X sample buffer, 3 sessions of 10 seconds sonication with cooling on ice water in between sessions, and 10 minutes boiling. Samples were loaded and resolved on precast 4-15% gradient SDS-PAGE gels and transferred to PVDF membrane as recommend by the manufacturer (Bio-Rad). On immunoblots, human TDP-43 was detected by a monoclonal antibody, anti-TDP-43 (ab57105[2E2-D3] Abcam, 1:10,000). TDP-43 phosphorylated at pS409/S410 was detected by a monoclonal antibody, anti-phospho TDP-43 (pS409/410, TIP-PTD-M01, Cosmobio, 1:667). Human tau was detected by a polyclonal antibody anti-tau (A0024, Dako, 1:200,000). Phosphorylated tau was detected by a monoclonal antibody anti-phosphorylated tau (AT8/PHF-Tau, MN1020, Thermo, 1:1000). *C. elegans* β-tubulin levels were measured using monoclonal antibody E7 (Developmental Studies Hybridoma Bank, 1:5000) as a loading control. HRP-labeled goat anti-mouse IgG secondary antibody (Jackson ImmunoResearch) was used at a dilution of 1:2500. HRP-labeled mouse anti-rabbit IgG secondary antibody (Jackson ImmunoResearch) was used at a dilution of 1:10,000. Quantitation was completed by ImageJ software densitometry analysis of scanned film images.

Statistical analyses

All statistical analyses were performed using GraphPad Prism statistical software. Statistical significance was determined using one-way ANOVA with Tukey's multiple-comparison test. Behavioral assays are graphed using violin plots; all other data are presented using standard bar graphs. Error bars represent standard error of the mean (SEM).

Availability of data and materials: The datasets used and/or analyzed during the current study are included in this published article and its supplementary information files are available from the corresponding author on reasonable request.

Acknowledgements: We thank the reviewers for helpful comments and suggestions. We thank Aleen Saxton, Aristide Black, and Brandon Henderson for outstanding technical assistance. We thank the Developmental Studies Hybridoma Bank (NICHD) for the β-tubulin antibody E7. Some strains were provided by the CGC, which is funded by NIH Office of Research Infrastructure Programs (P40 OD010440). We thank WormBase for model organism information and resources. This material is the result of work supported with resources and the use of facilities at the VA Puget Sound Health Care System.

Competing interests: The authors declare that they have no competing interests.

Funding: This work was supported by grants from the United States (U.S.) Department of Veterans Affairs (VA) Biomedical Laboratory Research and Development Service [Merit Review Grant #I01BX004044 (NFL)] and National Institutes of Health [K08AG065426 (CSL), R01AG066729 (NFL), R01NS064131 (BCK)], and the Nancy and Buster Alvord Endowment (CDK).

Author contributions: CL conceived experiments, performed project administration and supervision, conducted *C. elegans* experiments, analyzed and interpreted data, and wrote the manuscript. JS conducted *C. elegans* experiments, analyzed and interpreted data, and wrote the manuscript. HC conducted *C. elegans* experiments, analyzed and interpreted data, and

wrote the manuscript. JH conducted *C. elegans* experiments, analyzed and interpreted data, and wrote the manuscript. TDB conceived experiments, analyzed and interpreted data, and wrote the manuscript. CDK conceived experiments, performed project administration and supervision, analyzed and interpreted data, and wrote the manuscript. BCK conceived experiments, performed project administration and supervision, analyzed and interpreted data, and wrote the manuscript. NFL conceived experiments, performed project administration and supervision, conducted *C. elegans* experiments, analyzed and interpreted data, and wrote the manuscript. All authors read and approved the final manuscript.

References:

1. Mirra, S. S. *et al.* The Consortium to Establish a Registry for Alzheimer's Disease (CERAD): Part II. Standardization of the neuropathologic assessment of Alzheimer's disease. *Neurology* (1991) doi:10.1212/WNL.41.4.479.
2. Braak, H. & Braak, E. *Neuropathological stageing of Alzheimer-related changes*. *Acta Neuropathologica* (1991). doi:10.1007/BF00308809.
3. Braak, H., Alafuzoff, I., Arzberger, T., Kretzschmar, H. & Tredici, K. Staging of Alzheimer disease-associated neurofibrillary pathology using paraffin sections and immunocytochemistry. *Acta Neuropathol. (Berl.)* (2006) doi:10.1007/s00401-006-0127-z.
4. Thal, D. R., Rüb, U., Orantes, M. & Braak, H. Phases of Aβ-deposition in the human brain and its relevance for the development of AD. *Neurology* (2002) doi:10.1212/WNL.58.12.1791.
5. Hyman, B. T. *et al.* National Institute on Aging-Alzheimer's Association guidelines for the neuropathologic assessment of Alzheimer's disease. *Alzheimers Dement. J. Alzheimers Assoc.* **8**, 1–13 (2012).

6. Latimer, C. S., Lucot, K. L., Keene, C. D., Cholerton, B. & Montine, T. J. Genetic Insights into Alzheimer's Disease. *Annu. Rev. Pathol.* **16**, 351–376 (2021).
7. Nelson, P. T. *et al.* Correlation of Alzheimer disease neuropathologic changes with cognitive status: a review of the literature. *J. Neuropathol. Exp. Neurol.* **71**, 362–381 (2012).
8. Chen, X.-Q. & Mobley, W. C. Alzheimer Disease Pathogenesis: Insights From Molecular and Cellular Biology Studies of Oligomeric Aβ and Tau Species. *Front. Neurosci.* **13**, 659 (2019).
9. Strang, K. H., Golde, T. E. & Giasson, B. I. MAPT mutations, tauopathy, and mechanisms of neurodegeneration. *Lab. Investig. J. Tech. Methods Pathol.* **99**, 912–928 (2019).
10. Busche, M. A. & Hyman, B. T. Synergy between amyloid-β and tau in Alzheimer's disease. *Nat. Neurosci.* **23**, 1183–1193 (2020).
11. Josephs, K. A. *et al.* TAR DNA-binding protein 43 and pathological subtype of Alzheimer's disease impact clinical features. *Ann. Neurol.* **78**, 697–709 (2015).
12. Josephs, K. A. *et al.* TDP-43 is a key player in the clinical features associated with Alzheimer's disease. *Acta Neuropathol. (Berl.)* **127**, 811–824 (2014).
13. Kapasi, A. *et al.* Limbic-predominant age-related TDP-43 encephalopathy, ADNC pathology, and cognitive decline in aging. *Neurology* **95**, e1951–e1962 (2020).
14. James, B. D. *et al.* TDP-43 stage, mixed pathologies, and clinical Alzheimer's-type dementia. *Brain J. Neurol.* **139**, 2983–2993 (2016).
15. Arai, T. *et al.* TDP-43 is a component of ubiquitin-positive tau-negative inclusions in frontotemporal lobar degeneration and amyotrophic lateral sclerosis. *Biochem. Biophys. Res. Commun.* (2006) doi:10.1016/j.bbrc.2006.10.093.

16. Neumann, M. *et al.* Ubiquitinated TDP-43 in frontotemporal lobar degeneration and amyotrophic lateral sclerosis. *Science* (2006) doi:10.1126/science.1134108.

17. Buratti, E. & Baralle, F. E. Multiple roles of TDP-43 in gene expression, splicing regulation, and human disease. *Front. Biosci. J. Virtual Libr.* **13**, 867–878 (2008).

18. Ratti, A. & Buratti, E. Physiological functions and pathobiology of TDP-43 and FUS/TLS proteins. *J. Neurochem.* **138 Suppl**, 95–111 (2016).

19. François-Moutal, L. *et al.* Structural Insights Into TDP-43 and Effects of Post-translational Modifications. *Front. Mol. Neurosci.* **12**, 301 (2019).

20. Kabashi, E. *et al.* Gain and loss of function of ALS-related mutations of TARDBP (TDP-43) cause motor deficits in vivo. *Hum. Mol. Genet.* (2009) doi:10.1093/hmg/ddp534.

21. Gao, J., Wang, L., Huntley, M. L., Perry, G. & Wang, X. Pathomechanisms of TDP-43 in neurodegeneration. *J. Neurochem.* (2018) doi:10.1111/jnc.14327.

22. Gendron, T. F., Rademakers, R. & Petrucelli, L. TARDBP mutation analysis in TDP-43 proteinopathies and deciphering the toxicity of mutant TDP-43. *J. Alzheimers Dis. JAD* **33 Suppl 1**, S35-45 (2013).

23. Van Deerlin, V. M. *et al.* TARDBP mutations in amyotrophic lateral sclerosis with TDP-43 neuropathology: a genetic and histopathological analysis. *Lancet Neurol.* **7**, 409–416 (2008).

24. Wang, I.-F., Wu, L.-S. & Shen, C.-K. J. TDP-43: an emerging new player in neurodegenerative diseases. *Trends Mol. Med.* **14**, 479–485 (2008).

25. Arai, T. *et al.* Phosphorylated TDP-43 in Alzheimer's disease and dementia with Lewy bodies. *Acta Neuropathol. (Berl.)* **117**, 125–136 (2009).

26. Amador-Ortiz, C. *et al.* TDP-43 immunoreactivity in hippocampal sclerosis and Alzheimer's disease. *Ann. Neurol.* **61**, 435–445 (2007).

27. Jung, Y. *et al.* TDP-43 in Alzheimer's disease is not associated with clinical FTLD or Parkinsonism. *J. Neurol.* **261**, 1344–1348 (2014).

28. Nag, S. *et al.* TDP-43 pathology in anterior temporal pole cortex in aging and Alzheimer's disease. *Acta Neuropathol. Commun.* **6**, 33 (2018).

29. Keage, H. A. D. *et al.* TDP-43 pathology in the population: prevalence and associations with dementia and age. *J. Alzheimers Dis. JAD* **42**, 641–650 (2014).

30. Uryu, K. *et al.* Concomitant TAR-DNA-binding protein 43 pathology is present in Alzheimer disease and corticobasal degeneration but not in other tauopathies. *J. Neuropathol. Exp. Neurol.* **67**, 555–564 (2008).

31. Kadokura, A., Yamazaki, T., Lemere, C. A., Takatama, M. & Okamoto, K. Regional distribution of TDP-43 inclusions in Alzheimer disease (AD) brains: their relation to AD common pathology. *Neuropathol. Off. J. Jpn. Soc. Neuropathol.* **29**, 566–573 (2009).

32. Josephs, K. A. *et al.* Abnormal TDP-43 immunoreactivity in AD modifies clinicopathologic and radiologic phenotype. *Neurology* **70**, 1850–1857 (2008).

33. Josephs, K. A. *et al.* Staging TDP-43 pathology in Alzheimer's disease. *Acta Neuropathol. (Berl.)* **127**, 441–450 (2014).

34. Josephs, K. A. *et al.* Protein contributions to brain atrophy acceleration in Alzheimer's disease and primary age-related tauopathy. *Brain J. Neurol.* **143**, 3463–3476 (2020).

35. Latimer, C. S. *et al.* Resistance and resilience to Alzheimer's disease pathology are associated with reduced cortical pTau and absence of limbic-predominant age-related TDP-43 encephalopathy in a community-based cohort. *Acta Neuropathol. Commun.* **7**, 91 (2019).

36. Chang, X.-L., Tan, M.-S., Tan, L. & Yu, J.-T. The Role of TDP-43 in Alzheimer's Disease. *Mol. Neurobiol.* **53**, 3349–3359 (2016).

37. Josephs, K. A. *et al.* Rates of hippocampal atrophy and presence of post-mortem TDP-43 in patients with Alzheimer's disease: a longitudinal retrospective study. *Lancet Neurol.* **16**, 917–924 (2017).

38. Kapasi, A. *et al.* Limbic-predominant age-related TDP-43 encephalopathy, ADNC pathology, and cognitive decline in aging. *Neurology* **95**, e1951–e1962 (2020).

39. James, B. D. *et al.* TDP-43 stage, mixed pathologies, and clinical Alzheimer's-type dementia. *Brain J. Neurol.* **139**, 2983–2993 (2016).

40. Josephs, K. A. *et al.* Rates of hippocampal atrophy and presence of post-mortem TDP-43 in patients with Alzheimer's disease: a longitudinal retrospective study. *Lancet Neurol.* **16**, 917–924 (2017).

41. Higashi, S. *et al.* Concurrence of TDP-43, tau and alpha-synuclein pathology in brains of Alzheimer's disease and dementia with Lewy bodies. *Brain Res.* **1184**, 284–294 (2007).

42. Smith, V. D. *et al.* Overlapping but distinct TDP-43 and tau pathologic patterns in aged hippocampi. *Brain Pathol. Zurich Switz.* **28**, 264–273 (2018).

43. Gu, J. *et al.* TDP-43 suppresses tau expression via promoting its mRNA instability. *Nucleic Acids Res.* (2017) doi:10.1093/nar/gkx175.

44. Montalbano, M. *et al.* TDP-43 and Tau Oligomers in Alzheimer's Disease, Amyotrophic Lateral Sclerosis, and Frontotemporal Dementia. *Neurobiol. Dis.* **146**, 105130 (2020).

45. Wurmthaler, L. A., Sack, M., Gense, K., Hartig, J. S. & Gamerdinger, M. A tetracycline-dependent ribozyme switch allows conditional induction of gene expression in Caenorhabditis elegans. *Nat. Commun.* **10**, 491 (2019).

46. Kraemer, B. C. *et al.* Neurodegeneration and defective neurotransmission in a Caenorhabditis elegans model of tauopathy. *Proc. Natl. Acad. Sci.* (2003) doi:10.1073/pnas.1533448100.

47. Wolozin, B., Gabel, C., Ferree, A., Guillily, M. & Ebata, A. Watching worms whither: Modeling neurodegeneration in C. elegans. *Prog. Mol. Biol. Transl. Sci.* (2011) doi:10.1016/B978-0-12-384878-9.00015-7.

48. Fong, S. *et al.* Energy crisis precedes global metabolic failure in a novel Caenorhabditis elegans Alzheimer Disease model. *Sci. Rep.* **6**, 33781 (2016).

49. Brignull, H. R., Moore, F. E., Tang, S. J. & Morimoto, R. I. Polyglutamine proteins at the pathogenic threshold display neuron-specific aggregation in a pan-neuronal Caenorhabditis elegans model. *J. Neurosci. Off. J. Soc. Neurosci.* **26**, 7597–7606 (2006).

50. Guthrie, C. R., Schellenberg, G. D. & Kraemer, B. C. SUT-2 potentiates tau-induced neurotoxicity in Caenorhabditis elegans. *Hum. Mol. Genet.* (2009) doi:10.1093/hmg/ddp099.

51. Liachko, N. F. *et al.* The phosphatase calcineurin regulates pathological TDP-43 phosphorylation. *Acta Neuropathol. (Berl.)* (2016) doi:10.1007/s00401-016-1600-y.

52. Kraemer, B. C., Burgess, J. K., Chen, J. H., Thomas, J. H. & Schellenberg, G. D. Molecular pathways that influence human tau-induced pathology in Caenorhabditis elegans. *Hum. Mol. Genet.* (2006) doi:10.1093/hmg/ddl067.

53. Miyasaka, T. *et al.* Progressive neurodegeneration in C. elegans model of tauopathy. *Neurobiol. Dis.* (2005) doi:10.1016/j.nbd.2005.03.017.

54. Guha, S., Fischer, S., Johnson, G. V. W. & Nehrke, K. Tauopathy-associated tau modifications selectively impact neurodegeneration and mitophagy in a novel C. elegans single-copy transgenic model. *Mol. Neurodegener.* **15**, 65 (2020).

55. Pir, G. J., Choudhary, B. & Mandelkow, E. Caenorhabditis elegans models of tauopathy. *FASEB J. Off. Publ. Fed. Am. Soc. Exp. Biol.* **31**, 5137–5148 (2017).

56. Liu, H. *et al.* Reciprocal modulation of 5-HT and octopamine regulates pumping via feedforward and feedback circuits in C. elegans. *Proc. Natl. Acad. Sci.* **116**, 7107 (2019).

57. Lockery, S. R. *et al.* A microfluidic device for whole-animal drug screening using electrophysiological measures in the nematode C. elegans. *Lab. Chip* **12**, 2211–2220 (2012).

58. Wheeler, J. M., Guthrie, C. R. & Kraemer, B. C. The role of MSUT-2 in tau neurotoxicity: a target for neuroprotection in tauopathy? *Biochem Soc Trans* (2010) doi:10.1042/BST0380973.

59. Guthrie, C. R., Greenup, L., Leverenz, J. B. & Kraemer, B. C. MSUT2 is a determinant of susceptibility to tau neurotoxicity. *Hum. Mol. Genet.* (2011) doi:10.1093/hmg/ddr079.

60. de Boer, E. M. J. *et al.* TDP-43 proteinopathies: a new wave of neurodegenerative diseases. *J. Neurol. Neurosurg. Psychiatry* **92**, 86–95 (2020).

61. Arseni, D. *et al.* Structure of pathological TDP-43 filaments from ALS with FTLD. *Nature* (2021) doi:10.1038/s41586-021-04199-3.

62. Clippinger, A. K. *et al.* Robust cytoplasmic accumulation of phosphorylated TDP-43 in transgenic models of tauopathy. *Acta Neuropathol. (Berl.)* **126**, 39–50 (2013).

63. Taylor, S. R. *et al.* Molecular topography of an entire nervous system. *Cell* **184**, 4329-4347.e23 (2021).

64. Saxena, S. & Caroni, P. Selective neuronal vulnerability in neurodegenerative diseases: from stressor thresholds to degeneration. *Neuron* **71**, 35–48 (2011).

65. Francis, P. T. The interplay of neurotransmitters in Alzheimer's disease. *CNS Spectr.* **10**, 6–9 (2005).

66. Cheng, Y.-J., Lin, C.-H. & Lane, H.-Y. Involvement of Cholinergic, Adrenergic, and Glutamatergic Network Modulation with Cognitive Dysfunction in Alzheimer's Disease. *Int. J. Mol. Sci.* **22**, (2021).

67. Cowburn, R., Hardy, J., Roberts, P. & Briggs, R. Presynaptic and postsynaptic glutamatergic function in Alzheimer's disease. *Neurosci. Lett.* **86**, 109–113 (1988).

68. McEntee, W. J. & Crook, T. H. Glutamate: its role in learning, memory, and the aging brain. *Psychopharmacology (Berl.)* **111**, 391–401 (1993).

69. Etienne, P. *et al.* Nucleus basalis neuronal loss, neuritic plaques and choline acetyltransferase activity in advanced Alzheimer's disease. *Neuroscience* **19**, 1279–1291 (1986).

70. Wevers, A. & Schröder, H. Nicotinic acetylcholine receptors in Alzheimer's disease. *J. Alzheimers Dis. JAD* **1**, 207–219 (1999).

71. Mattson, M. P. Involvement of GABAergic interneuron dysfunction and neuronal network hyperexcitability in Alzheimer's disease: Amelioration by metabolic switching. *Int. Rev. Neurobiol.* **154**, 191–205 (2020).

72. Xu, Y., Zhao, M., Han, Y. & Zhang, H. GABAergic Inhibitory Interneuron Deficits in Alzheimer's Disease: Implications for Treatment. *Front. Neurosci.* **14**, 660 (2020).

73. Ruan, Z. *et al.* Alzheimer's disease brain-derived extracellular vesicles spread tau pathology in interneurons. *Brain J. Neurol.* **144**, 288–309 (2021).

74. Trillo, L. *et al.* Ascending monoaminergic systems alterations in Alzheimer's disease. translating basic science into clinical care. *Neurosci. Biobehav. Rev.* **37**, 1363–1379 (2013).

75. Šimić, G. *et al.* Monoaminergic neuropathology in Alzheimer's disease. *Prog. Neurobiol.* **151**, 101–138 (2017).

76. Sennik, S., Schweizer, T. A., Fischer, C. E. & Munoz, D. G. Risk Factors and Pathological Substrates Associated with Agitation/Aggression in Alzheimer's Disease: A Preliminary Study using NACC Data. *J. Alzheimers Dis. JAD* **55**, 1519–1528 (2017).

77. Elferink, M. W.-O., van Tilborg, I. & Kessels, R. P. C. Perception of emotions in mild cognitive impairment and Alzheimer's dementia: does intensity matter? *Transl. Neurosci.* **6**, 139–149 (2015).

78. Simic, G. *et al.* Does Alzheimer's disease begin in the brainstem? *Neuropathol. Appl. Neurobiol.* **35**, 532–554 (2009).

79. Benbow, S. J., Strovas, T. J., Darvas, M., Saxton, A. & Kraemer, B. C. Synergistic toxicity between tau and amyloid drives neuronal dysfunction and neurodegeneration in transgenic C. elegans. *Hum. Mol. Genet.* **29**, 495–505 (2020).

80. Power, M. C. *et al.* Combined neuropathological pathways account for age-related risk of dementia. *Ann. Neurol.* **84**, 10–22 (2018).

81. Teipel, S. J., Temp, A. G. M., Levin, F., Dyrba, M. & Grothe, M. J. Association of TDP-43 Pathology with Global and Regional 18F-Florbetapir PET Signal in the Alzheimer's Disease Spectrum. *J. Alzheimers Dis. JAD* **79**, 663–670 (2021).

82. Hicks, D. A., Jones, A. C., Pickering-Brown, S. M. & Hooper, N. M. The cellular expression and proteolytic processing of the amyloid precursor protein is independent of TDP-43. *Biosci. Rep.* **40**, (2020).

83. Laos, V. *et al.* Catalytic Cross Talk between Key Peptide Fragments That Couple Alzheimer's Disease with Amyotrophic Lateral Sclerosis. *J. Am. Chem. Soc.* **143**, 3494–3502 (2021).

84. Shih, Y.-H. *et al.* TDP-43 interacts with amyloid-β, inhibits fibrillization, and worsens pathology in a model of Alzheimer's disease. *Nat. Commun.* **11**, 5950 (2020).

85. Kraemer, B. C. & Schellenberg, G. D. SUT-1 enables tau-induced neurotoxicity in C. elegans. *Hum. Mol. Genet.* (2007) doi:10.1093/hmg/ddm143.

86. Kow, R. L. *et al.* Distinct Poly(A) nucleases have differential impact on sut-2 dependent tauopathy phenotypes. *Neurobiol. Dis.* **147**, 105148 (2021).

87. McMillan, P. J. *et al.* Pathological tau drives ectopic nuclear speckle scaffold protein SRRM2 accumulation in neuron cytoplasm in Alzheimer's disease. *Acta Neuropathol. Commun.* **9**, 117 (2021).

88. Grenier St-Sauveur, V., Soucek, S., Corbett, A. H. & Bachand, F. Poly(A) tail-mediated gene regulation by opposing roles of Nab2 and Pab2 nuclear poly(A)-binding proteins in pre-mRNA decay. *Mol. Cell. Biol.* **33**, 4718–4731 (2013).

89. Kampers, T., Friedhoff, P., Biernat, J., Mandelkow, E. M. & Mandelkow, E. RNA stimulates aggregation of microtubule-associated protein tau into Alzheimer-like paired helical filaments. *FEBS Lett.* **399**, 344–349 (1996).

90. Ginsberg, S. D., Crino, P. B., Lee, V. M., Eberwine, J. H. & Trojanowski, J. Q. Sequestration of RNA in Alzheimer's disease neurofibrillary tangles and senile plaques. *Ann. Neurol.* **41**, 200–209 (1997).

91. Chornenkyy, Y., Fardo, D. W. & Nelson, P. T. Tau and TDP-43 proteinopathies: kindred pathologic cascades and genetic pleiotropy. *Lab. Investig. J. Tech. Methods Pathol.* **99**, 993–1007 (2019).

92. Tomé, S. O. *et al.* TDP-43 interacts with pathological τ protein in Alzheimer's disease. *Acta Neuropathol. (Berl.)* (2021) doi:10.1007/s00401-021-02295-2.

93. Bukar Maina, M., Al-Hilaly, Y. K. & Serpell, L. C. Nuclear Tau and Its Potential Role in Alzheimer's Disease. *Biomolecules* **6**, 9 (2016).

94. Lin, W.-L. & Dickson, D. W. Ultrastructural localization of TDP-43 in filamentous neuronal inclusions in various neurodegenerative diseases. *Acta Neuropathol. (Berl.)* **116**, 205–213 (2008).

95. White, M. A. *et al.* TDP-43 gains function due to perturbed autoregulation in a Tardbp knock-in mouse model of ALS-FTD. *Nat. Neurosci.* **21**, 552–563 (2018).

96. Gu, J. *et al.* Transactive response DNA-binding protein 43 (TDP-43) regulates alternative splicing of tau exon 10: Implications for the pathogenesis of tauopathies. *J. Biol. Chem.* **292**, 10600–10612 (2017).

97. Hortobágyi, T. & Cairns, N. J. Amyotrophic lateral sclerosis and non-tau frontotemporal lobar degeneration. *Handb. Clin. Neurol.* **145**, 369–381 (2017).

98. Tan, R. H., Ke, Y. D., Ittner, L. M. & Halliday, G. M. ALS/FTLD: experimental models and reality. *Acta Neuropathol. (Berl.)* **133**, 177–196 (2017).

99. Brenner, S. Nature's gift to science (Nobel lecture). *Chembiochem Eur. J. Chem. Biol.* **4**, 683–687 (2003).

100. Wu, Y. *et al.* Amyloid-beta-induced pathological behaviors are suppressed by Ginkgo biloba extract EGb 761 and ginkgolides in transgenic Caenorhabditis elegans. *J. Neurosci. Off. J. Soc. Neurosci.* **26**, 13102–13113 (2006).

101. McIntire, S. L., Reimer, R. J., Schuske, K., Edwards, R. H. & Jorgensen, E. M. Identification and characterization of the vesicular GABA transporter. *Nature* **389**, 870–876 (1997).

102. Liachko, N. F., Guthrie, C. R. & Kraemer, B. C. Phosphorylation Promotes Neurotoxicity in a Caenorhabditis elegans Model of TDP-43 Proteinopathy. *J. Neurosci.* (2010) doi:10.1523/JNEUROSCI.2911-10.2010.

Figures

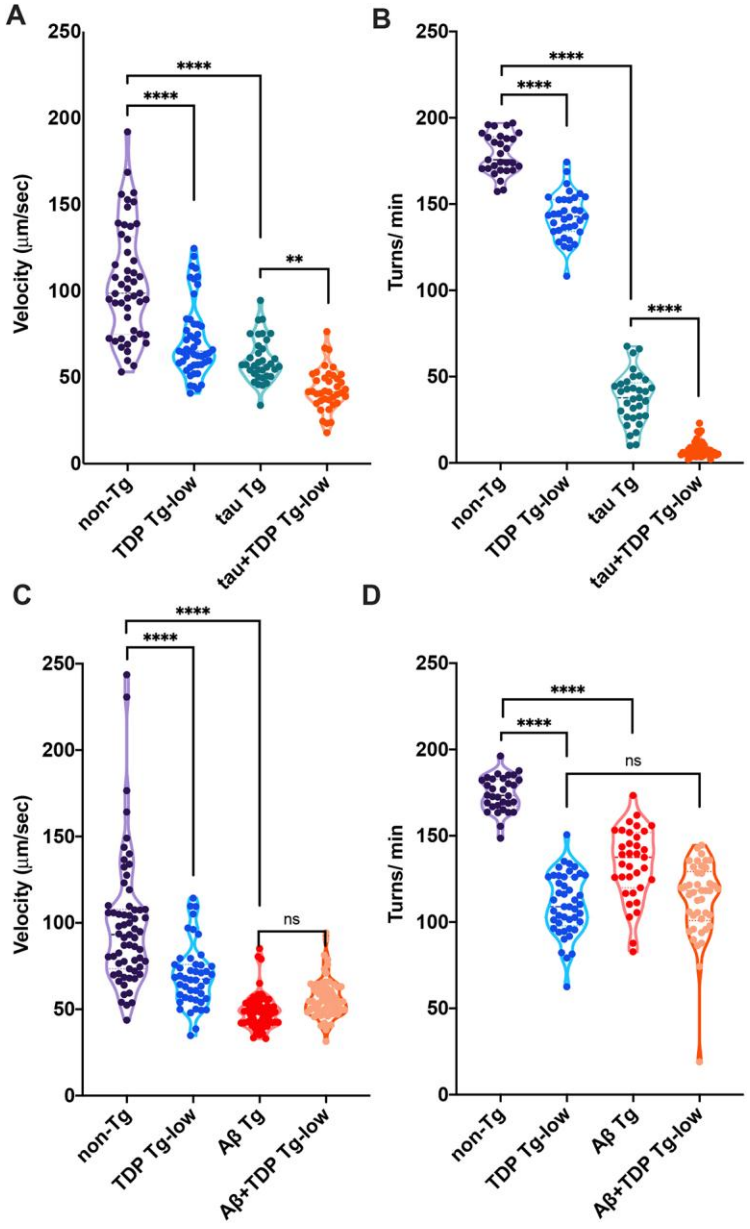

Figure 1: Co-expression of TDP-43 with tau but not Aβ leads to enhancement of motility deficits. a tau+TDP Tg-low have significantly decreased activity. Unstimulated activity on a seeded agar plate is detected using unbiased computer-assisted video tracking and analysis. Movement (velocity) was recorded (µm/sec). ****p<0.0001. N=115 (non-TG), 66 (TDP Tg-low), 89 (tau Tg), 93 (tau+TDP Tg-low), from 3 independent replicates. **b** tau+TDP Tg-low have

significantly decreased thrashing in liquid. Rates of thrashing were measured using unbiased computer-assisted tracking and analysis. The number of turns (thrashes) per minute were recorded (turns/ min). ****p<0.0001. N=73 (non-TG), 89 (TDP Tg-low), 81 (tau Tg), 87 (tau+TDP Tg-low), from 3 independent replicates. **c** Unstimulated activity on a seeded agar plate is detected using unbiased computer-assisted video tracking and analysis. Movement (velocity) was recorded (µm/sec). ****p<0.0001. ns=not significant. N=147 (non-TG), 119 (TDP Tg-low), 163 (Aβ Tg), 182 (Aβ+TDP Tg-low), from 3 independent replicates. **d** Rates of thrashing in liquid were measured using unbiased computer-assisted tracking and analysis. The number of turns (thrashes) per minute were recorded (turns/ min). ns=not significant, ****p<0.0001. N=85 (non-TG), 105 (TDP Tg-low), 101 (Aβ Tg), 119 (Aβ+TDP Tg-low), from 3 independent replicates.

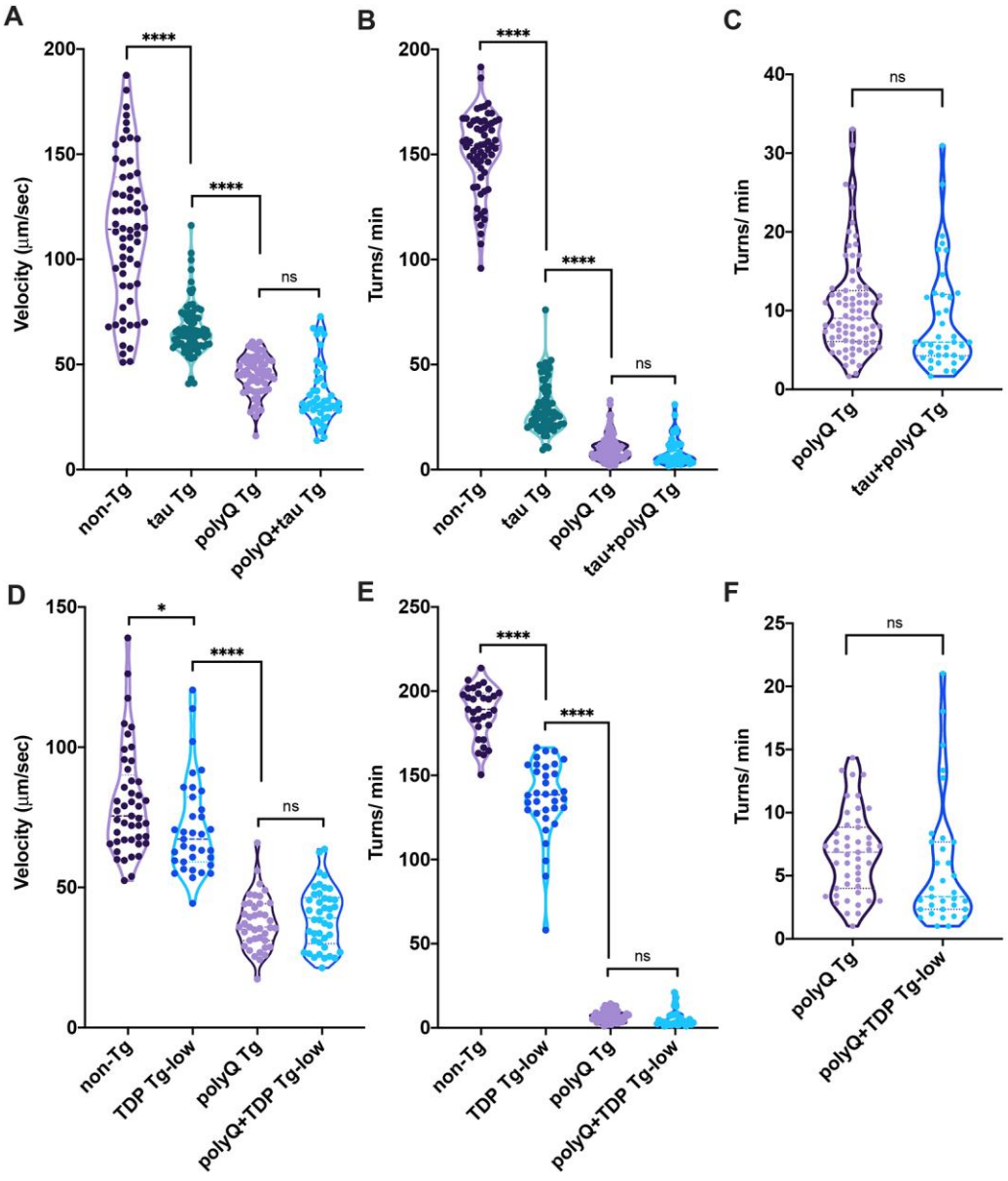

Figure 2: tau and TDP-43 do not synergize with poly-glutamine. a-c tau does not synergize with poly-glutamine. **a** Unstimulated activity on a seeded agar plate is detected using unbiased computer-assisted video tracking and analysis. Movement (velocity) was recorded (µm/ sec). ****p<0.0001. ns=not significant. N=140 (non-TG), 179 (tau Tg), 138 (polyQ Tg), 110 (polyQ+tau Tg), from 3 independent replicates. **b** Rates of thrashing in liquid were measured using unbiased computer-assisted tracking and analysis. The number of turns (thrashes) per minute were recorded (turns/ min). ns=not significant, ****p<0.0001. N=149 (non-TG), 204 (tau Tg), 167 (polyQ Tg), 132 (polyQ+tau Tg), from 3 independent replicates. **c** Data from **(b)** with

decreased y-axis to allow visual comparisons between polyQ Tg and tau+polyQ Tg strains. **d-f** TDP-43 does not synergize with poly-glutamine. **c** Unstimulated activity on a seeded agar plate is detected using unbiased computer-assisted video tracking and analysis. Movement (velocity) was recorded (µm/ sec).*p<0.05, ****p<0.0001. ns=not significant. N=123 (non-TG), 99 (TDP Tg-low), 116 (polyQ Tg), 87 (polyQ+TDP Tg-low), from 3 independent replicates. **d** Rates of thrashing in liquid were measured using unbiased computer-assisted tracking and analysis. The number of turns (thrashes) per minute were recorded (turns/ min). ns=not significant, ****p<0.0001. N=82 (non-TG), 94 (TDP Tg-low), 116 (polyQ Tg), 83 (polyQ+TDP Tg-low), from 3 independent replicates. **f** Data from **(e)** with decreased y-axis to allow visual comparisons between polyQ Tg and TDP+polyQ Tg strains.

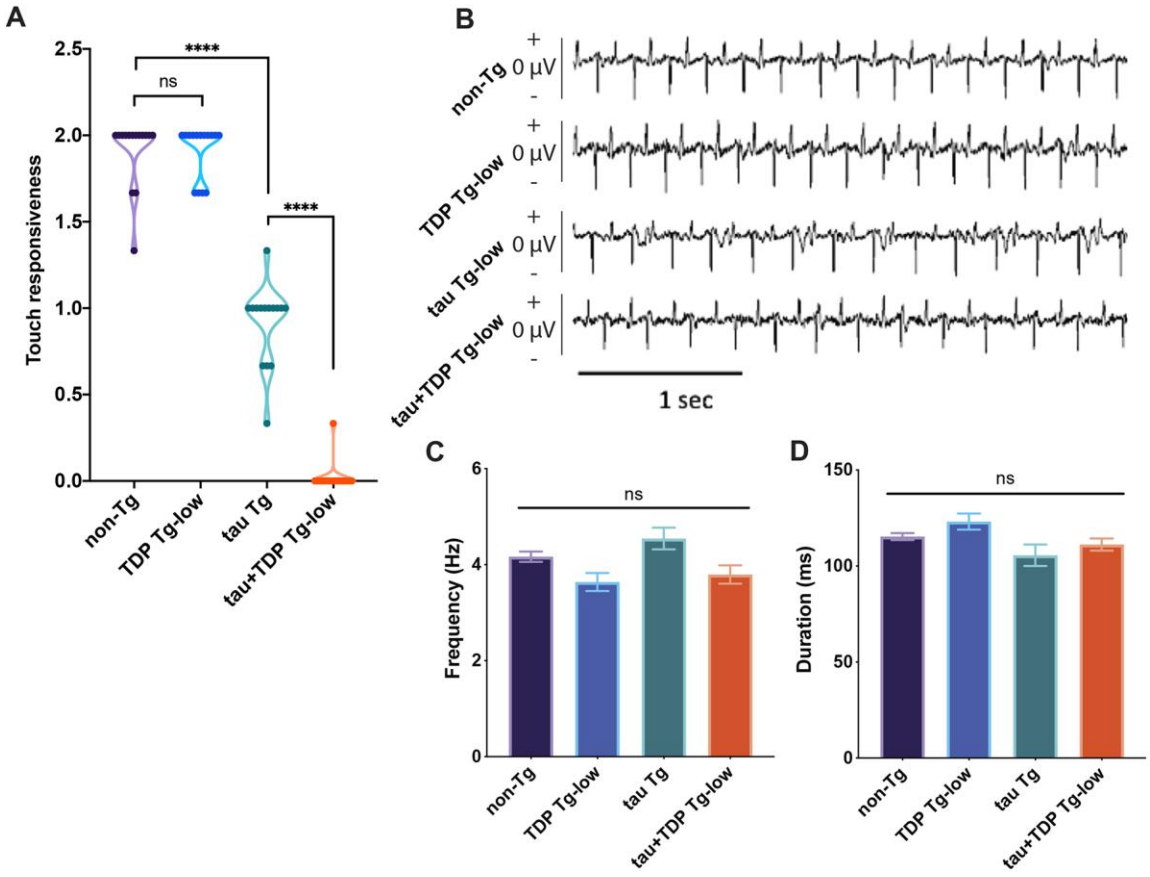

Figure 3: tau+TDP Tg-low exhibit mechanosensory defects but intact pharyngeal pumping. a tau+TDP Tg-low animals have significantly worse mechanosensation. Mechanosensation was assayed by responsiveness to a light touch, and scored as 2: normal response, 1: abnormal response, or 0: no response. ns=not significant, ****p<0.0001. N=45 (all strains), from 3 independent replicates. **b-d** *C. elegans* pharyngeal pumping was evaluated by recording pharyngeal muscle and neuron action potentials to generate an electropharyngeogram (EPG). No significant differences were detected among strains. **b** Representative EPG traces of pharyngeal action potentials showing both positive (excitatory) and negative (relaxation) spikes. **c** Average pump frequency and **d** average pump duration over a 2 minute recording. N=39 (non-TG), 36 (TDP Tg-low), 32 (tau Tg), 35 (tau+TDP Tg-low), from 3 independent replicates. ns= not significant.

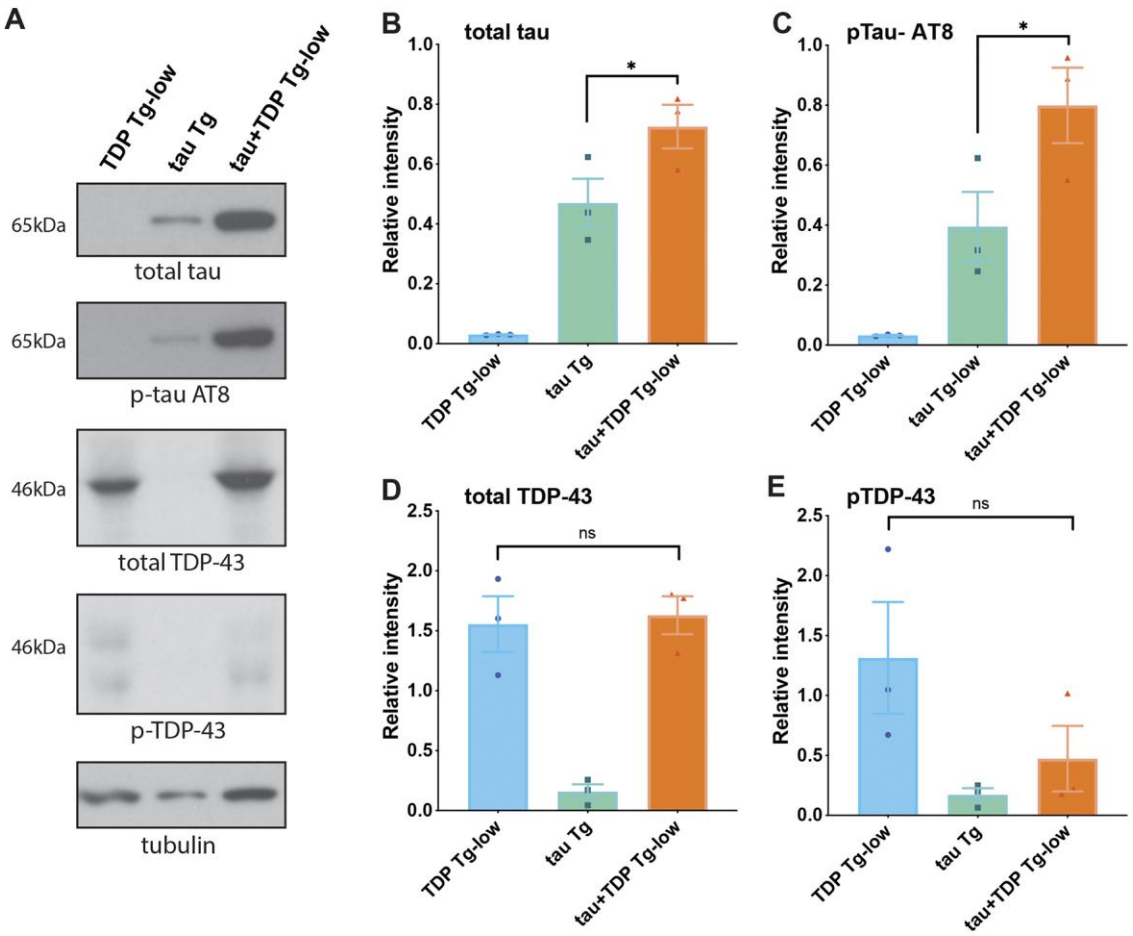

Figure 4: tau and TDP-43 co-expression promotes accumulation and phosphorylation of tau. Developmentally synchronized day 1 adult *C. elegans* were harvested and tested by immunoblot for total tau, phosphorylated tau (AT8), total TDP-43, phosphorylated TDP-43 (phospho-S409/410) and tubulin (load control). **a** Immunoblot shown is representative of three independent replicate experiments **b-e**, Quantification of protein levels normalized to tubulin. Total tau (**b**) and phosphorylated tau (**c**) are elevated in tau+TDP-low Tg animals. Total TDP-43 (**d**) and phosphorylated TDP-43 (**e**) are not elevated in tau+TDP-low Tg animals. (*$p < 0.05$; ns = not significant).

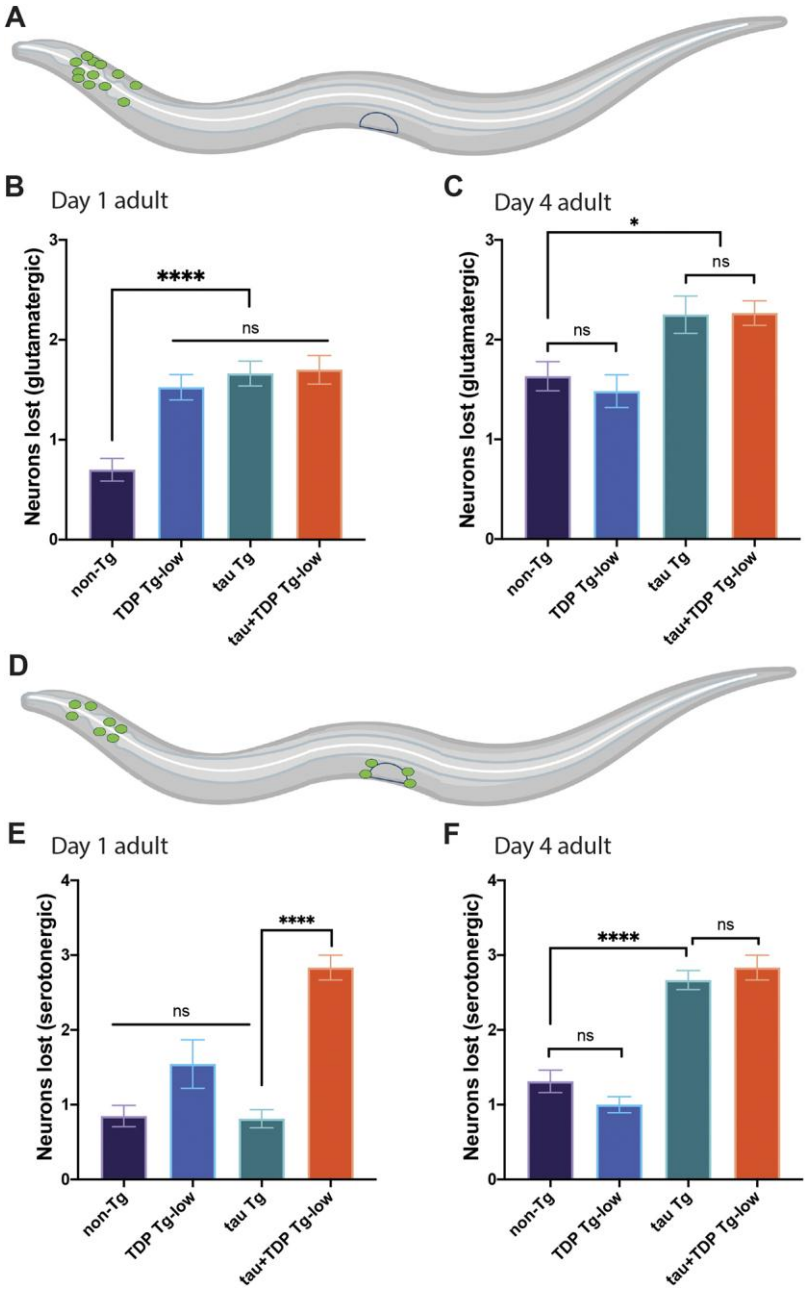

Figure 5: Co-expression of tau and TDP-43 leads to selective glutamatergic and serotonergic neurodegeneration. a-c Assessment of glutamatergic neurons in tau+TDP Tg-low animals. **a** Depiction of neurons scored (green). **b** Quantification of neurons lost in developmentally synchronized day 1 adult (**b**) and day 4 adult (**c**) *C. elegans.* ns = not significant, $^{**}p < 0.01$; $^{****}p < 0.0001$). N>40 for all strains and timepoints scored, from at least 3 independent replicates. **d-f** Assessment of serotonergic neurons in tau+TDP Tg-low animals. **d** Depiction of

neurons scored (green). **e-f** Quantification of neurons lost in developmentally synchronized day 1 adult (**e**) and day 4 adult (**f**) *C. elegans.* ns = not significant, ****$p < 0.0001$). N>45 for all strains and timepoints scored, from at least 3 independent replicates.

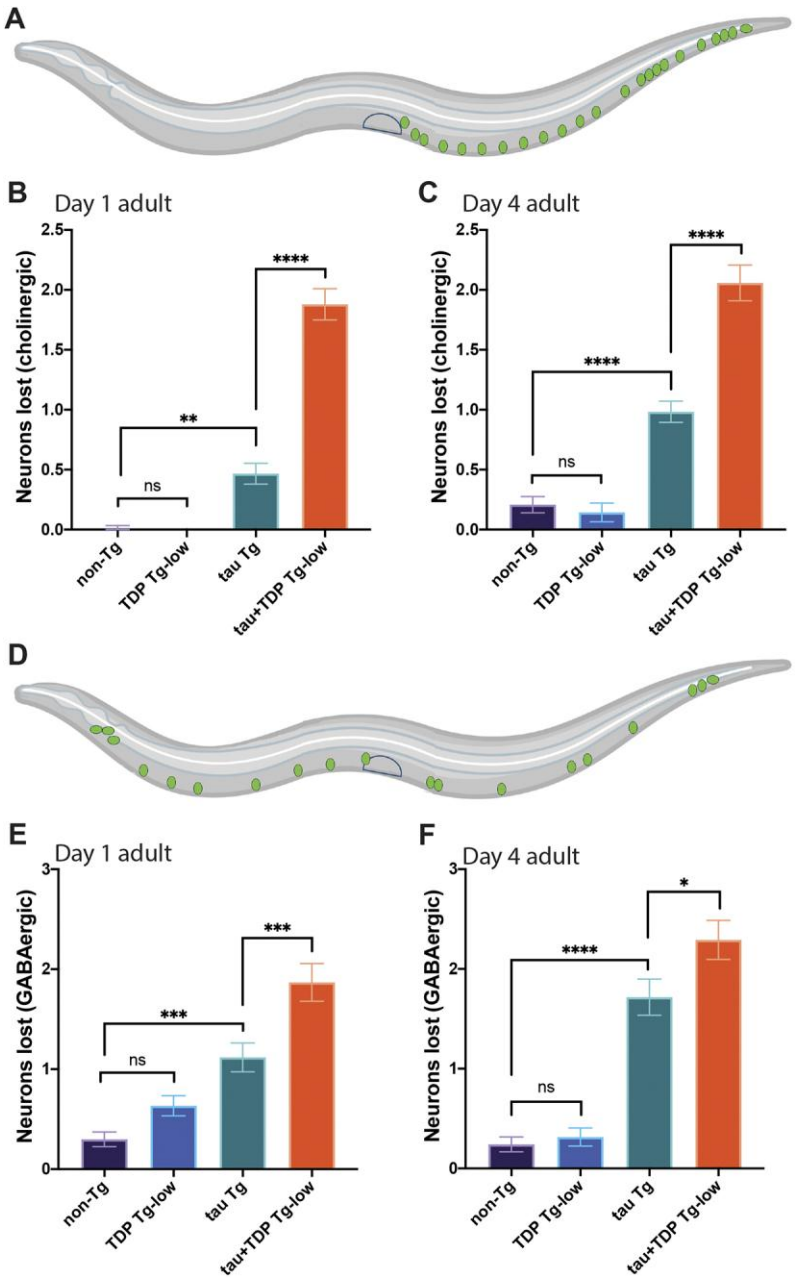

Figure 6: Co-expression of tau and TDP-43 leads to selective cholinergic and GABA-ergic neurodegeneration. a-c Assessment of cholinergic neurons in tau+TDP Tg-low animals. **a** Depiction of neurons scored (green). **b** Quantification of neurons lost in developmentally synchronized day 1 adult (**b**) and day 4 adult (**c**) *C. elegans.* ns = not significant, $^{**}p < 0.01$; $^{****}p < 0.0001$). N>45 for all strains and timepoints scored, from at least 3 independent replicates. **d-f** Assessment of GABA-ergic neurons in tau+TDP Tg-low animals. **d** Depiction of

neurons scored (green). **e-f** Quantification of neurons lost in developmentally synchronized day 1 adult (**e**) and day 4 adult (**f**) *C. elegans.* ns = not significant, *$p < 0.05$; *** $p < 0.001$; ****$p < 0.0001$). N>45 for all strains and timepoints scored, from at least 3 independent replicates.

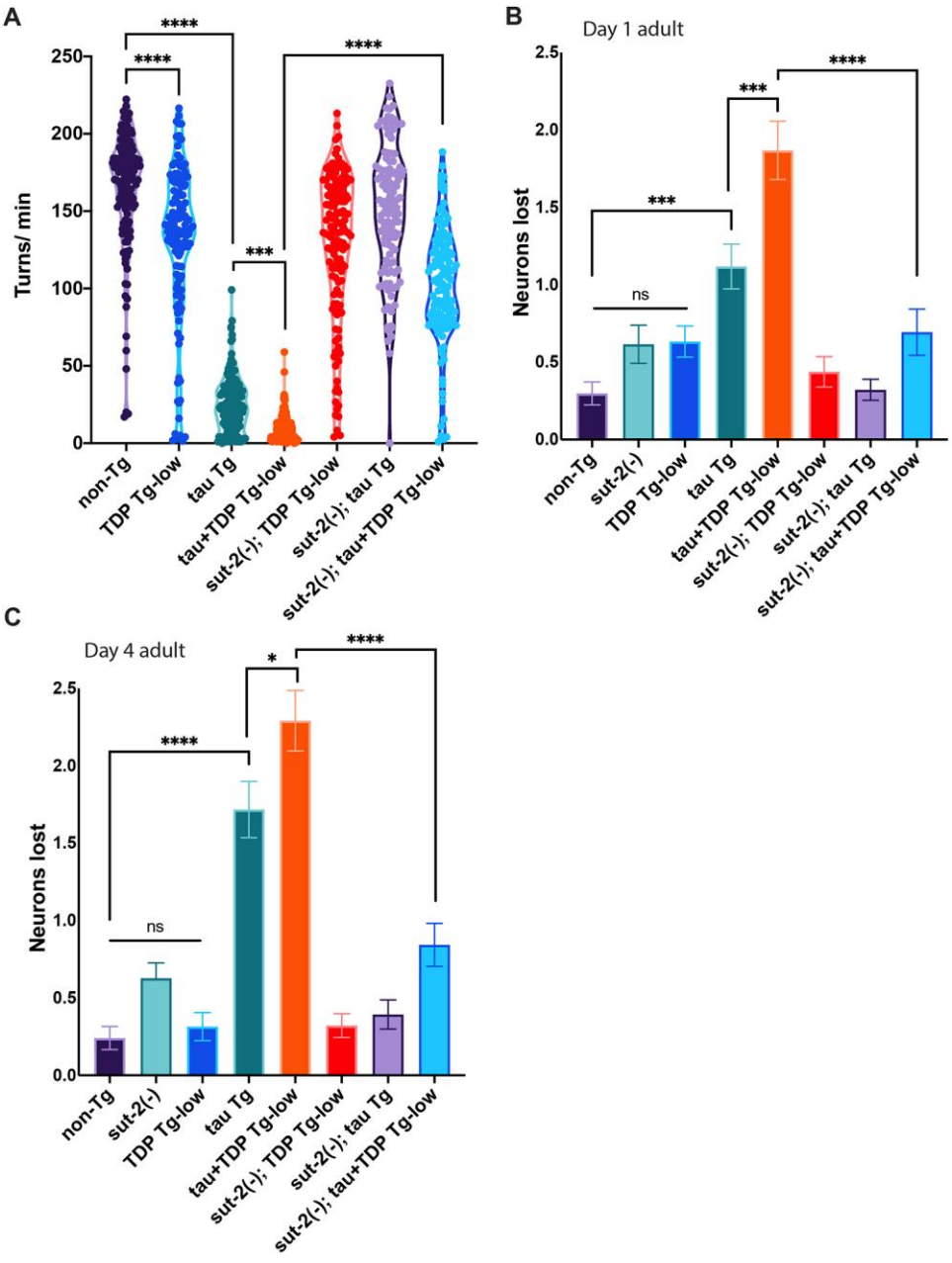

Figure 7: Loss of *sut-2* expression prevents motility deficits and neurodegeneration in a model of combined tau and TDP-43 expression. a tau+TDP Tg-low have significantly decreased thrashing in liquid, which is rescued by *sut-2(-)*. Rates of thrashing were measured using unbiased computer-assisted tracking and analysis. The number of turns (thrashes) per minute were recorded (turns/ min). ***p<0.0008, ****p<0.0001. TDP-43 Tg-low *vs sut-2(-);* TDP Tg-low: p=0.9833, tau Tg *vs sut-2(-)*; tau Tg: p<0.0001, tau+TDP Tg-low *vs sut-2(-);* tau+TDP Tg-low:

p<0.0001. N=149 (non-TG), 134 (TDP Tg-low), 167 (tau Tg), 185 (tau+TDP Tg-low), 145 (*sut-2(-);* TDP Tg-low), 121 (*sut-2(-)*; tau Tg), 131 (*sut-2(-);* tau+TDP Tg-low) from 3 independent replicates. Error bars represent SD. **b-c** Quantification of neurons lost in developmentally synchronized day 1 adult (**b**) and day 4 adult (**c**) *C. elegans* show that *sut-2(-)* prevents neuron loss in tau+TDP Tg-low animals. ns = not significant, *$p < 0.05$; ***$p < 0.001$; ****$p < 0.0001$). (**b**) TDP-43 Tg-low *vs sut-2(-);* TDP Tg-low: p=0.9504, tau Tg *vs sut-2(-)*; tau Tg: p=0.0002, tau+TDP Tg-low *vs sut-2(-);* tau+TDP Tg-low: p<0.0001. (**c**) TDP-43 Tg-low *vs sut-2(-);* TDP Tg-low: p>0.9999, tau Tg *vs sut-2(-)*; tau Tg: p<0.0001, tau+TDP Tg-low *vs sut-2(-);* tau+TDP Tg-low: p<0.0001. N>45 for all strains and timepoints scored, from at least 3 independent replicates.

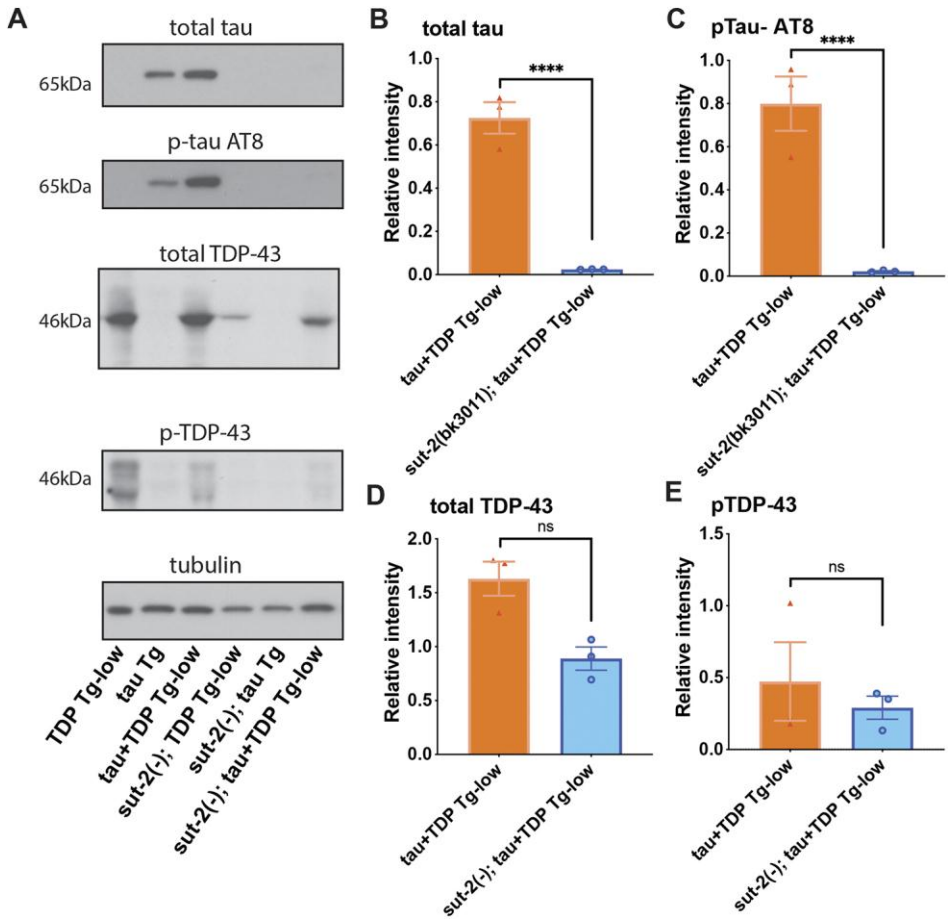

Figure 8: Loss of *sut-2* expression prevents tau protein accumulation in a model of combined tau and TDP-43 expression. a-e Developmentally synchronized day 1 adult *C. elegans* were harvested and tested by immunoblot for total tau, phosphorylated tau (AT8), total TDP-43, phosphorylated TDP-43 (phospho-S409/410) and tubulin (load control). **a** Immunoblot shown is representative of three independent replicate experiments **b-e** Quantification of protein levels performed by ImageJ software analysis of scanned film images. Total tau (**b**) and phosphorylated tau (**c**) are reduced in *sut-2(-);* tau+TDP-low Tg animals. Total TDP-43 (ns, p=0.0917) (**d**) and phosphorylated TDP-43 (**e**) are not significantly reduced in *sut-2(-)*; tau+TDP-low Tg animals. (*p < 0.05; ns = not significant).

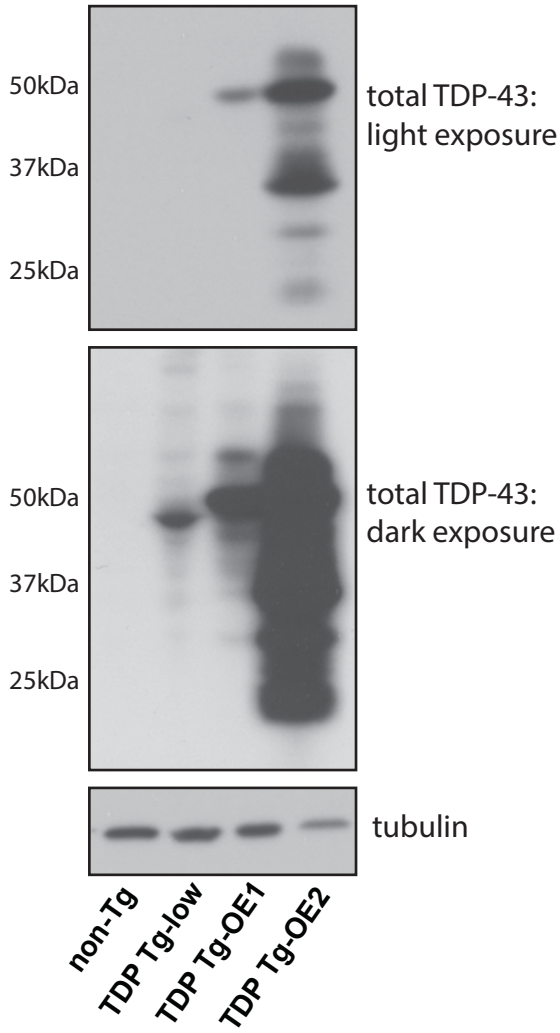

Fig. S1. TDP Tg-low animals express low levels of TDP-43. Immunoblot comparing TDP-43 protein levels among non-transgenic (non-Tg), TDP Tg-low, a TDP-43 transgenic line with moderate overexpression (TDP Tg-OE1), and a TDP-43 transgenic line with high levels of overexpression (TDP Tg-OE2). The TDP-43 sequence in each strain was verified by sequencing to code for full-length wild-type TDP-43. The slightly lower molecular weight of TDP Tg-low may be due to a lack of post-translational modifications, particularly phosphorylated TDP-43, which are present in the higher copy TDP-43 strains.

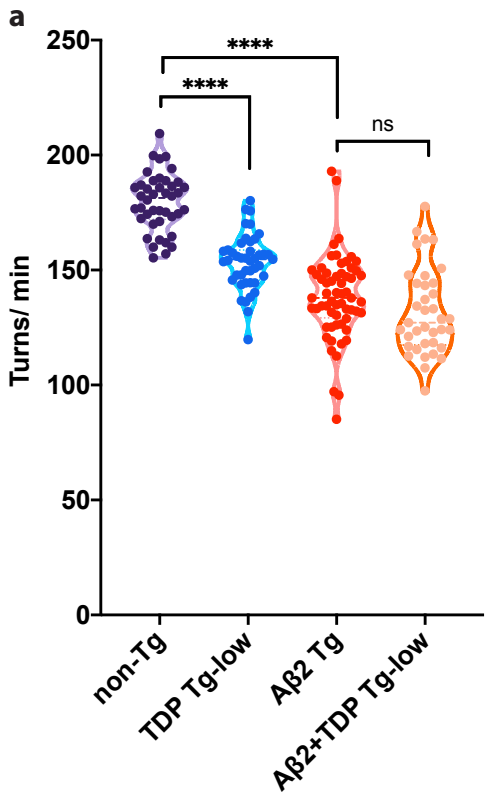

Fig. S2. tau+TDP Tg-low animals do not synergize with Aβ. a Rates of thrashing in liquid were measured using unbiased computer-assisted tracking and analysis. The number of turns (thrashes) per second were recorded (turns/ sec). ns=not significant, ****p<0.0001. N=128 (non-TG), 202 (TDP Tg-low), 140 (Aβ Tg), 97 (Aβ+TDP Tg-low), from 3 independent replicates. ****p<0.0001, ns=not significant.

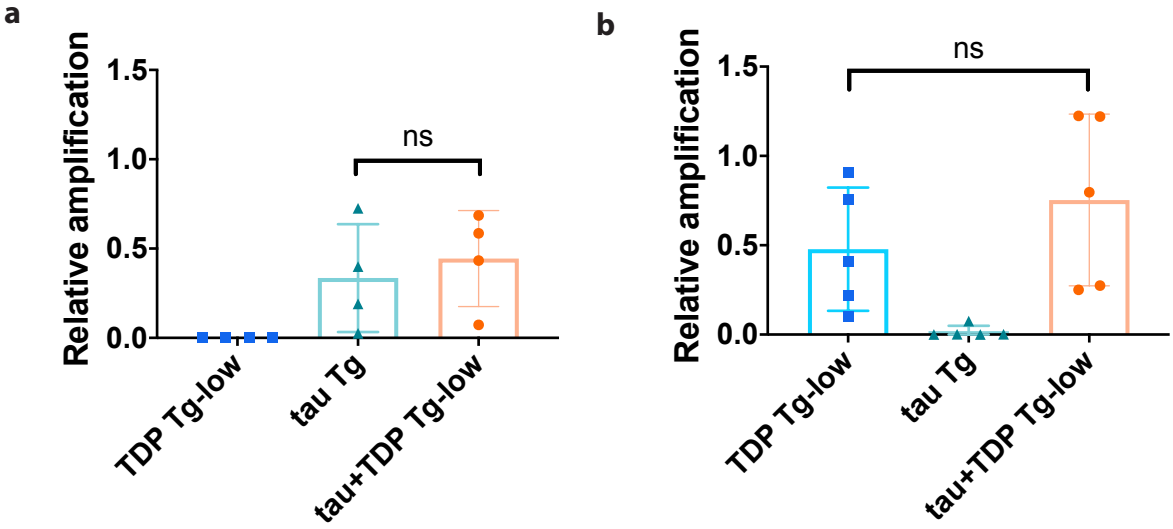

Fig. S3. mRNA expression of tau and TDP-43 transgenes are unchanged in tau +TDP-43 Tg-low. a Quantitative reverse-transcription PCR (qRT-PCR) testing expression of the tau transgene. tau signal is normalized to expression of an internal control gene, *rpl-32*, and plotted as arbitrary units. **b** qRT-PCR testing expression of the TDP-43 transgene. TDP-43 signal is normalized to expression of an internal control gene, *rpl-32*, and plotted as arbitrary units. ns=not significant.

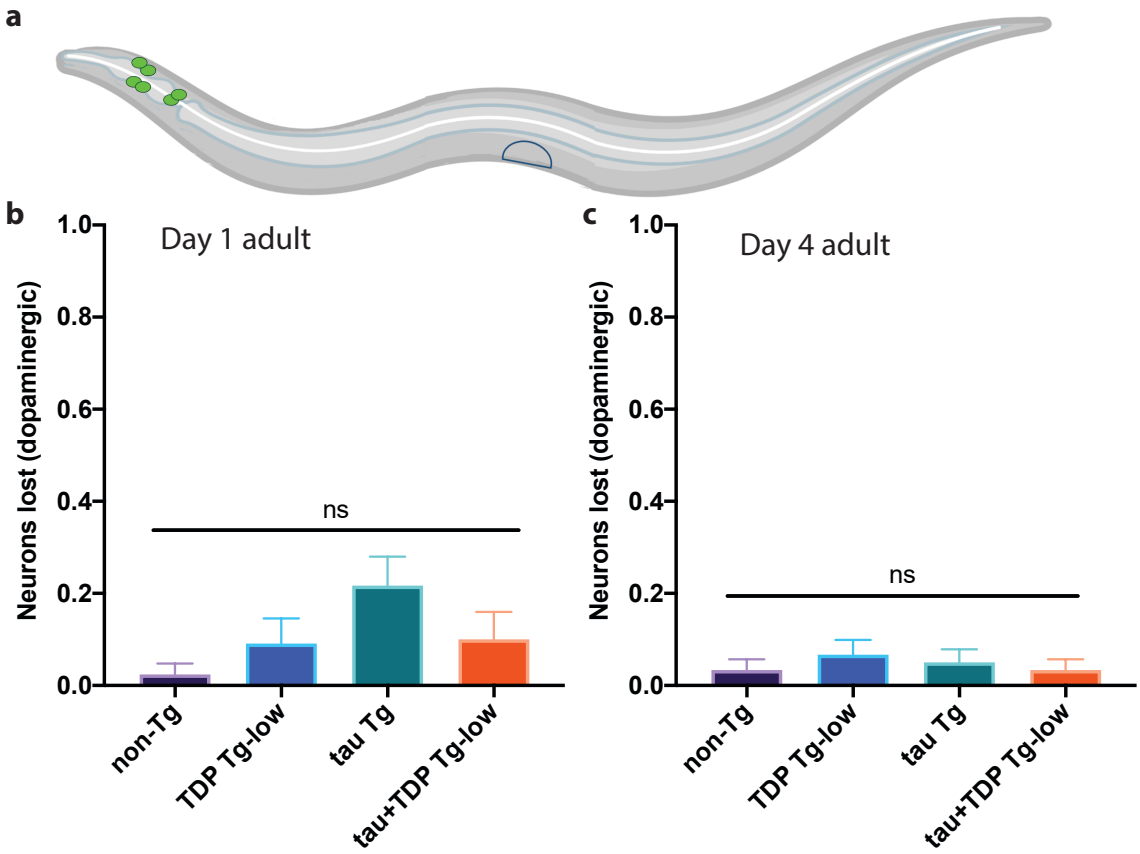

Fig. S4. Co-expression of tau and TDP-43 does not impact dopaminergic neurons. **a-c** Assessment of dopaminergic neurons in tau+TDP Tg-low animals. **a** Depiction of neurons scored (green). **b** Quantification of neurons lost in developmentally synchronized day 1 adult (**b**) and day 4 adult (**c**) *C. elegans*. ns = not significant. N>45 for all strains and timepoints scored, from at least 3 independent replicates.

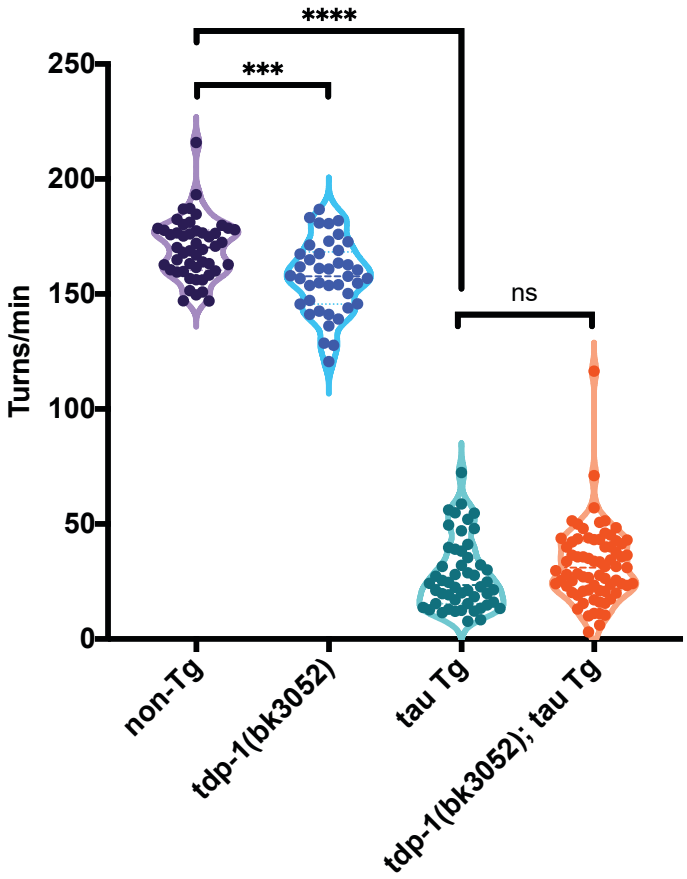

Fig. S5. Loss of the *C. elegans* homolog of TDP-43, *tdp-1*, does not alter tau-driven motility dysfunction. Rates of thrashing were measured using unbiased computer-assisted tracking and analysis. The number of turns (thrashes) per minute were recorded (turns/ min). ns=not significant, ***P<0.001, ****p<0.0001. N=49 (non-TG), 41 (*tdp-1(bk3052)*), 52 (tau Tg), 73 (*tdp-1(bk3052*); tau Tg), from 3 independent replicates.

Table S1. Strains used in this study.

Abbreviation	Strain name	Genotype	Transgene
non-Tg	N2	wild-type	
tau Tg	CK1441	*bkIs1441[Paex-3::Tau WT(4R1N)+Pmyo-2::dsRED]*	human tau
Aβ Tg	GRU102	*gnaIs2[Pmyo-2::YFP+Punc-119::Abeta1-42]*	human Aβ
Aβ Tg 2	CL2355	*dvIs50[pCL45(snb-1::Abeta1-42::3'UTR(long) + mlt-2::GFP]*	human Aβ
polyQ Tg	CK241	*bkIs241[pF25B5.3::Q86-YFP]*	86 repeats of glutamine
TDP Tg-low	CK1943	*[Psnb-1::hTDP-43 WT::K4aptazyme::unc-54 3'UTR+Pmyo-3::mCherry]*	human TDP-43
tau+TDP Tg-low	NLS19	*bkIs1441[Paex-3::Tau WT(4R1N)+Pmyo-2::dsRED]; bkIs1943[Psnb-1::hTDP-43 WT::K4aptazyme::unc-54 3'UTR+Pmyo-3::mCherry]*	human tau and TDP-43
sut-2(-); tau+TDP Tg-low	NLS23	*sut-2(bk3011); bkIs1441[Paex-3::Tau WT(4R1N)+Pmyo-2::dsRED]; bkIs1943[Psnb-1::hTDP-43 WT::K4aptazyme::unc-54 3'UTR+Pmyo-3::mCherry]*	human tau and TDP-43
sut-2(-); TDP Tg-low	NLS24	*sut-2(bk3011); bkIs1943[Psnb-1::hTDP-43 WT::K4aptazyme::unc-54 3'UTR+Pmyo-3::mCherry]*	human TDP-43
sut-2(-); tau Tg	NLS25	*sut-2(bk3011); bkIs1441[Paex-3::Tau WT(4R1N)+Pmyo-2::dsRED]*	human tau
	EG1285	*oxIs12*[P*unc-47*::GFP + *lin-15(+)*]	GABAergic neuron GFP
	JPS617	P*tph-1*::GFP	serotonergic neuron GFP
	WG1	P*dat-1*::GFP	dopaminergic neuron GFP
	OH10972	P*eat-4*::GFP	glutamatergic neuron GFP
	LX929	P*unc-17*::GFP	cholinergic neuron GFP
	CK3052	*tdp-1(bk3052)*	